Scientific Research Publishing

Open Journal of Geology, 2025, 15(3), 109-141
https://www.scirp.org/journal/ojg
ISSN Online: 2161-7589
ISSN Print: 2161-7570

Petrographic and Geochemical Study of Mantle Spinel Lherzolitic Xenoliths within Alkaline Hosted Lavas of Cenozoic Volcanism in the Head of the Cape Verde Peninsula (Senegal)

Abdoulaye Ndiaye[1], Mahamadane Diène[2], Papa Malick Ngom[1]

[1]Département de Géologie, Faculté des Sciences et Techniques, UCAD, Dakar, Sénégal
[2]Ecole Nationale Supérieure des Mines et de la Géologie ESMG (ex IST), Dakar, Sénégal
Email: abdoulaye152.ndiaye@ucad.edu.sn, mahamadane.diene@ucad.edu.sn, komalick@gmail.com

How to cite this paper: Ndiaye, A., Diène, M. and Ngom, P.M. (2025) Petrographic and Geochemical Study of Mantle Spinel Lherzolitic Xenoliths within Alkaline Hosted Lavas of Cenozoic Volcanism in the Head of the Cape Verde Peninsula (Senegal). *Open Journal of Geology*, **15**, 109-141.
https://doi.org/10.4236/ojg.2025.153005

Received: January 8, 2025
Accepted: March 8, 2025
Published: March 11, 2025

Abstract

Tertiary and quaternary Cenozoic alkaline-hosted lavas of the Senegal Cape Verde Peninsula have incorporated spinel lherzolitic xenoliths. The aim of this study is to characterize the petrography and geochemistry of these spinel lherzolitic xenoliths to better understand their original characteristics and the evolution of the mantle under the Senegal Cape Verde Peninsula. To achieve this objective, field mapping was conducted, and xenoliths were selected and sampled. Thin sections were prepared for petrographical and mineralogical analysis, and whole rocks were used for geochemical studies. The petrographical results show that the spinel lherzolitic xenoliths, ranging in size from 1.5 to 10 cm, are rounded to sub-rounded and sometimes elongated, with a protogranular texture. They are characterized by the absence of recrystallization, intense mineral fracturing, intergranular mineral slippage, and magmatic infiltration acting as a contaminant. The mineralogical characteristics show homogeneity in the mineral phases, comparable to those of xenoliths from oceanic platforms and hotspot basalts, as well as sub-continental fertile peridotites from island arcs. The main mineralogical phases are olivine and pyroxenes (orthopyroxenes and clinopyroxenes), associated with an aluminous spinel phase. The proportion of these mineral phases classifies them as harzburgite, dunites or lherzolites. There is no trace of garnet, plagioclase, amphibole, or phlogopite minerals. The relationship between the xenoliths and the host lavas indicates that these xenoliths are not cumulates and are therefore not cogenetic with the host rocks, suggesting their residual character. Mg# values of the olivines (75.9 to 92.4) and the absence of zonation are characteristic of the lherzolitic xenoliths found in alkaline basalts worldwide. This is confirmed by Mg#

values (from 82.8 to 93.7) and the variations of CaO, Al_2O_3, Cr_2O_3, NiO, and TiO_2 in the clinopyroxenes and orthopyroxenes, as well as the ratios of Mg# (63.00% to 84.2%) and Cr# (18.05% to 41.98%) in the spinels. These characteristics reveal a textural and mineralogical homogeneity of these xenoliths originating from the mantle. The Rare Earth spectra of all xenoliths studied show a progressive decrease from Light Rare Earths (LREE) to intermediate Rare Earths (MREE) to Heavy Rare Earths (HREE). The xenoliths from the Senegal Cape Verde Peninsula originate from a Rare Earth-depleted spinel lherzolite mantle source zone. The low contents of incompatible elements (Ce, La), high Ni and Cr contents, and the Mg/(Mg + Fe) ratio in both olivines and spinel lherzolitic xenoliths, coupled with the positive anomaly of Ta and P and a negative anomaly in Ba, Th, K, Pb, U, and Hf, appear compatible with the partial melting process. The variations of highly incompatible elements (U and Rb) indicate these elements are not significantly affected by post-magmatic or secondary alteration processes. The petrographical and mineralogical variations, combined with the geochemical variations of major and trace elements in the whole rocks, are compatible with a low degree of partial melting in an enriched upper mantle, such as the lherzolitic type. The low Rare-Earth element enrichment of these spinel lherzolitic xenoliths could indicate a probable interaction between the upper peridotitic mantle and the host magmas. The presence of these spinel lherzolitic xenoliths is likely linked to the evolution of mantle plumes, as seen in the Cameroon line, Cape Verde archipelago, or elsewhere. The geochemical results also suggest that the crust under the Senegal Cape Verde peninsula may consist of a fertile mantle affected by a low degree of partial melting. This is controlled by Cenozoic tectonics, with deep fractures affecting the head of the Senegal Cape Verde peninsula and facilitating the rapid ascent of host magma.

Keywords

Cenozoic Volcanism—Spinel Lherzolitic Xenoliths—Partial Melting—Cape Verde Peninsula, Mamelle, Manual Cape, Madelen Island, Senegal

1. Introduction

Cenozoic volcanic rocks containing spinel lherzolitic xenoliths were deposited during Tertiary and Quaternary volcanism. Tertiary-age volcanism outcrops from the head of the Senegal Cape Verde Peninsula to the Thiès region [1]-[5] (**Figure 1**). It exhibits complex volcanic activity, forming tuffs (in dykes, pipes, or sills), lava intrusions in N-S oriented fractures, or basaltic flows. The various Tertiary facies include tuffs, nephelinites, basanites, dolerites, and gabbros.

Quaternary-age volcanism is confined to the head of the Senegal Cape Verde Peninsula [4]-[8] (**Figure 2**). It consists of a lower volcanic unit known from boreholes, a middle volcanic unit known from boreholes and outcrops, and an upper volcanic unit. The upper volcanic unit includes the main polygenic Mamelle unit, associated with secondary units like the adventitious Mermoz unit. The main pol-

ygenic Mamelle volcanic unit evolved through several phases of magmatic activity: a phreatomagmatic phase produced stratified pyroclastic products, a strombolian phase produced scoria and breccias with a magmatic lava base, and a fissural Hawaiian phase produced basanitic and doleritic lava flows. The rocks include scoria, breccia, basanite, and dolerite. The secondary adventitious apparatus at Mermoz consists of breccia, scoria, and a lake of basanitic lavas.

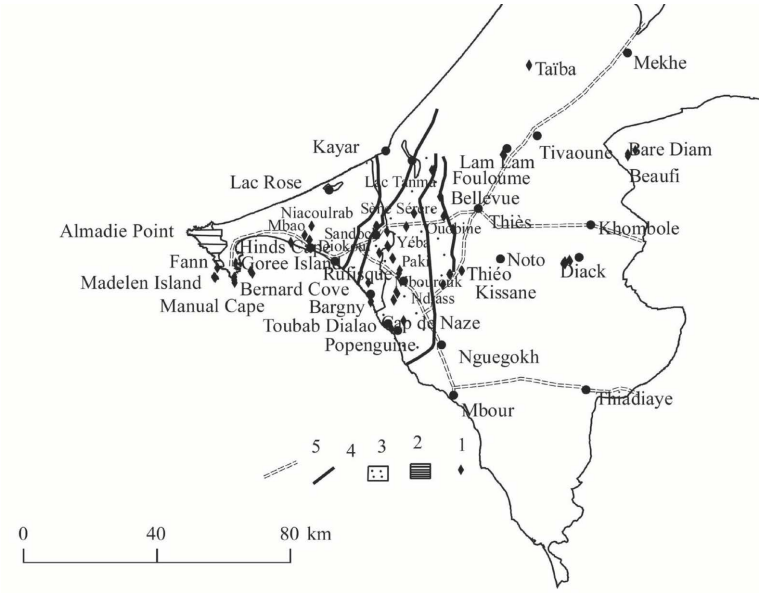

Figure 1. Location map of Tertiary and Quaternary volcanic rocks [13]. Legend: 1: Tertiary volcanism; 2: Quaternary volcanism; 3: Horst Ndiass; 4: Faults; 5: Access roads.

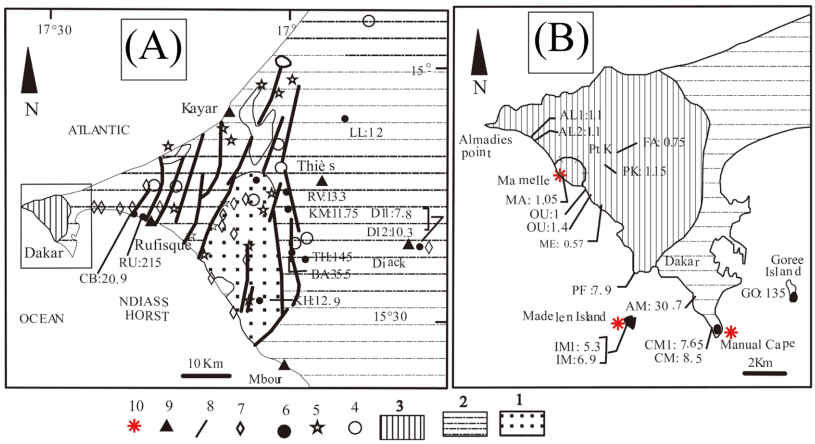

Figure 2. Outcrops of Cenozoic volcanic rocks in the Cap-Vert peninsula [4] in [14]: (A) Cap-Vert peninsula and Thiès areas; (B) The Cenozoic volcanism of the Cap-Vert peninsula head. 1: Mesozoic province (Ndiass Horst), 2: Tertiary, 3: Quaternary, 4: Outcrops of undated lavas, 5: Volcanic rocks found in drilling, 6: Outcrops of dated lavas (K-Ar ages in Ma), 7: Tuffs, 8: Faults, 9: Locality name, 10: red stars = Location of the sampling zone. CB = Hinds Cape; RU = Rufisque; LL = Lam-Lam; RV = Chieves Ravinee; KM = Keur Mamour; Th = Thiéo; BA = Bandia; KH = Khazabe; DI = Diack; AL = Almadies; MA = Mamelle; OU = Ouakam; Pt K = Point K; FA = Fort A; PF = Fann head; IM = Madelen Island; AM = Madelen Cove; CM = Manual Cape; GO = Gorée.

Tertiary volcanism is dated by K-Ar between 35.5 and 5.3 Ma, while Quaternary volcanism ranges from 1.5 to 0.57 Ma [4] [7]-[12] (**Figure 2**). The highly sodic, undersaturated lavas have an alkaline affinity and are weakly differentiated [2]-[5] [8] [13] [14]. The two volcanoes, Tertiary and Quaternary, are separated by a Fini-Tertiary lateritic alteration phase [5] [15] [16]. The volcanic area is located in the transition zone between oceanic and continental crust, which is affected by rifting-related tectonic breaking [4] [17]-[20].

Our study focuses on spinel lherzolitic xenoliths incorporated in alkaline volcanic rocks to demonstrate their characteristics, determine their origin, and understand the evolution of the mantle beneath the Senegal-Cape Verde Peninsula.

2. Methodology

The study involved bibliographical research, data collection in the field, and laboratory work. The fieldwork consisted of listing and describing the hosted bedrock exposures, and then systematically sampling the xenoliths to select the largest and freshest samples for this study. The fresh xenoliths studied were collected from Mamelle quaternary volcanism rocks (scoria, breccias, and glove-finger basanite) and in Manual Cape and Madelen Island tertiary volcanism rocks (prismatic basanite and nephelinite) (**Figure 2**). For each sample, one part was used for whole rock powders for major and trace elements analysis, and the other part was prepared to make thin sections.

For powder preparation, altered fragments or vein fillings were removed from the chips after crushing. The selected coarse chips were rinsed with deionized water and then dried. The samples were powdered and analyzed for bulk major and trace element concentrations. Whole-rock major and trace element compositions, as well as loss-on-ignition (LOI) values, were measured using X-ray fluorescence or the ICP-MS solution method at the Nancy Analysis Laboratory (France) according to the lab's standard operating procedures.

The thin section was prepared and analyzed in Clermont-Ferrand, France, and at Frederic II, Naples, Italy, for petrographic analysis. The major mineral element analysis was conducted using an electron microprobe (Camebax SX 50) in Clermont-Ferrand, France, to determine the composition of four mineral phases. Wavelength dispersive spectroscopy (WDS) was employed using an accelerating voltage of 20 kV, 15 nA, and a counting time of 20 seconds for each element. The details of the standards calibration, analytical accuracy, and precision have been assessed by analyzing natural and synthetic standards as defined by the labs.

3. Results

3.1. Petrography

3.1.1. Macroscopic Description of Spinel Lherzolitic Xenoliths

The sampling zone is located in Figure 2. The spinel lherzolitic xenoliths are light green, dense, generally subangular to sub-rounded, sometimes elongated, and shaped by the host lava. Their size ranges from 1.5 to 10 cm in length (**Figure**

3) and they are well preserved in the host lavas with coarse-grained olivines. The contact with the host lava is unambiguous, and the spinel lherzolitic xenoliths appear to be affected by the host lava, which can also infiltrate through their cracks. These spinel lherzolitic xenoliths might be residues of melting rock, removed and incorporated into the ascending host lava.

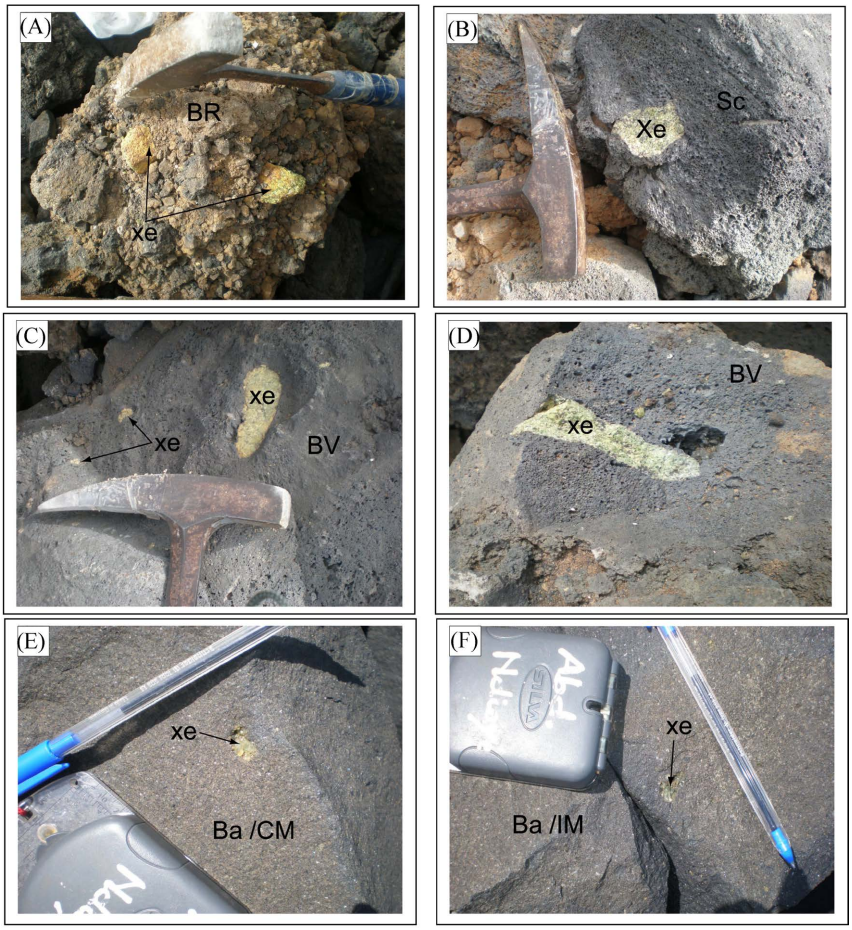

Figure 3. Macroscopic characteristics of greenish spinel lherzolitic xenoliths in Tertiary and Quaternary Mamelle lavas: Quaternary spinel lherzolitic xenoliths are found in volcanic breccia (A), Scoria (B), vesicular basanites (C) and (D); Tertiary spinel lherzolitic xenoliths in volcanic Manual Cape basanites (E), and Madelen Island basanites (F). Intact lherzolitic spinel xenoliths, detached and transported by the ascending host basalt, show clear contact with the host lava. Their structure features large olivine grains, typically about a millimeter in size. Br = Breccias; Xe = Xenoliths; Sc = Scoria; BV = Vesicular basanites; Ba/CM = Basanite of Manual Cape; Ba/IM = Basanite Madelen Island.

3.1.2. Microscopic Description of Spinel Lherzolitic Xenoliths

The textures observed in the spinel lherzolitic xenoliths studied are similar to the coarse-grained structure described in various alkali basalt xenoliths worldwide [21]. Currently, we have no recorded occurrences of garnet, plagioclase, phlogopite, or amphibole minerals described in various xenoliths worldwide.

The Quaternary spinel lherzolitic xenoliths from Mamelle are larger (3 to 7 cm)

and exhibit a protogranular structure (Figure 4(A)-(F); Figure 5(A) and Figure 5(B)). They consist of automorphic to subautomorphic minerals of olivine, pyroxene, and spinel.

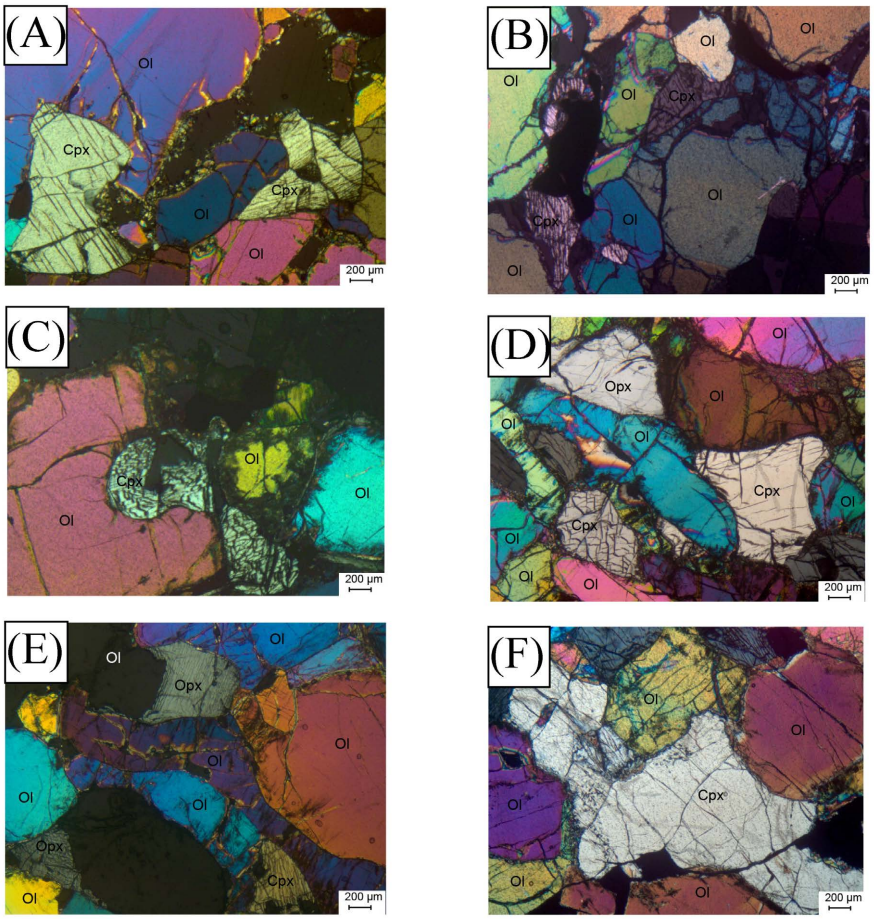

Figure 4. Analyzed polarized light micrographs of spinel lherzolitic xenoliths in Mamelle Quaternary lavas illustrate a protogranular texture. (A): Automorphic to subautomorphic olivines display numerous jointed minerals with triple points. Some crystals have irregular or rectilinear edges, while others are strongly cracked or have rounded contours, showing traces of dislocation and intergranular slippage. Automorphic to subautomorphic pyroxenes are interstitial between olivine minerals. (B): Automorphous to subautomorphous olivines are present. Some minerals are cracked, while others are elongated with intergranular slippage. Automorphous to subautomorphous pyroxenes are interstitial between olivine minerals. (C): Automorphous to subautomorphous olivines have curved or irregular boundaries. Note the rounded pyroxene partially embedded in the olivines. (D) and (E): The olivines are strongly elongated and fractured. Pyroxenes are interstitial between the olivine minerals. The minerals show numerous dislocations and intergranular sliding. (F): Subautomorphic pyroxenes are interstitial between automorphic and subautomorphic minerals. Legend: Ol = Olivine; Cpx = Clinopyroxene; Opx = Orthopyroxene.

The tertiary xenoliths from Manual Cape are small (2 to 5 cm) and composed of olivines, pyroxenes, and spinels. Xenoliths also have a protogranular texture (Figure 5(C)-(E)). Small olivine crystals are sometimes partially or totally embedded in pyroxenes.

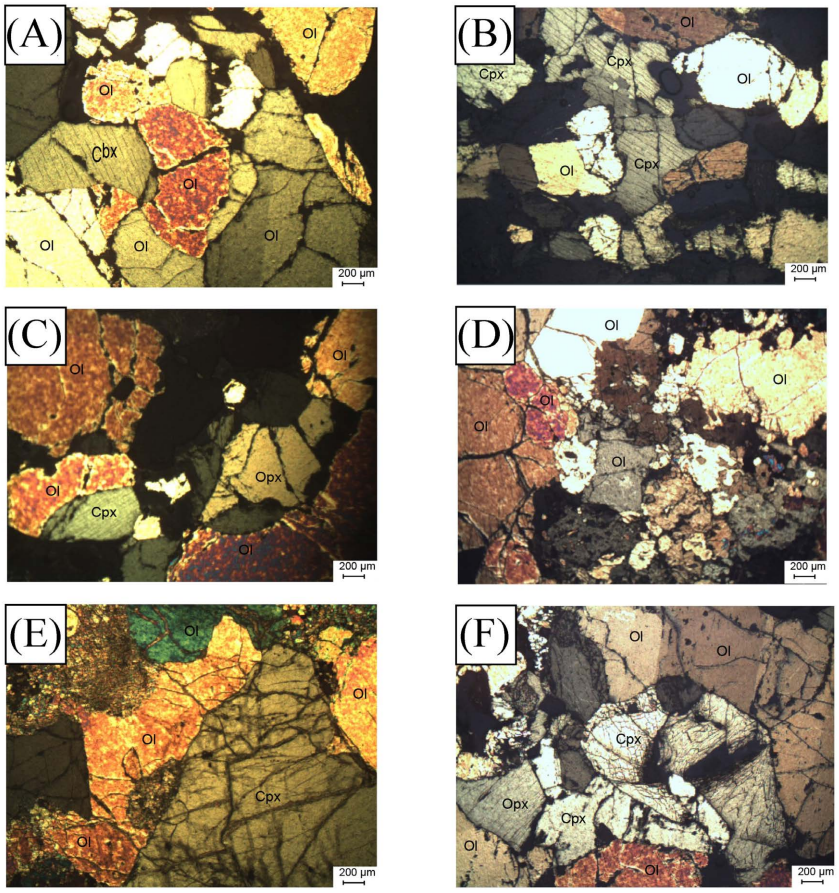

Figure 5. Analyzed polarized light micrographs of spinel lherzolitic xenoliths in Mamelle Quaternary lavas (A) and (B) and Tertiary Manual Cape (C), (D) and (E) and Madelen Island (F) lavas, illustrating the protogranular texture. (A): Mamelle Quaternary xenoliths. Strongly fractured automorphic to subautomorphic olivines with rectilinear or curved margins and automorphic interstitial pyroxenes. Note the elongation of some olivines and intergranular slippage. (B): Mamelle Quaternary xenoliths. Alignment of numerous subautomorphic pyroxenes forming patches between automorphic to subautomorphic olivine crystals. (C): Manual Cape Tertiary xenolith: subautomorphic olivine with curved or irregular boundaries, leaving spaces where subautomorphic pyroxenes crystallize. (D): Tertiary xenolith from Manual Cape composed mainly of olivine, showing two generations of olivine with irregular grain boundaries. (E): Manual Cape Tertiary xenolith of olivine partially embedded in irregular pyroxene rims. (F): Madelen Island Tertiary xenolith. Heavily fractured automorphic to subautomorphic olivine with rectilinear margins between which numerous subautomorphic interstitial pyroxenes crystallize. Note the intergranular slip. Legend: Ol = Olivine; Cpx = Clinopyroxene; Opx = Orthopyroxene.

Interstitial pyroxenes between olivines are destabilized by subsequent thermal disruption. In some areas, the minerals exhibit intergranular sliding and basaltic infiltration along fractures.

The Madelen Island xenoliths are found in prismatic basanites and are small (2 to 4 cm). They have a protogranular structure **Figure 5(F)**. Some minerals show a reaction aureole in contact with the host lava and intergranular sliding. They consist

mainly of olivine and pyroxene, with spinel being very rare. Olivine is fractured and shows intergranular sliding. Interstitial pyroxene is often associated with spinel. The spinel is vermicular, poly-lobed, elongated, or appears as small, aligned grains.

Automorphous to subautomorphous pyroxenes are interstitial and have been corroded near the contact with the host lava. Rectilinear or curvilinear boundaries defining polygonal junctions or triple junction points between olivine or olivine and pyroxene phases indicate that these xenoliths are close to textural equilibrium (**Figure 6(A)** and **Figure 6(B)**). Some minerals are partially or totally altered, with a reaction aureole around the contact between hosted rocks and xenoliths (**Figures 6(C)-(F)**).

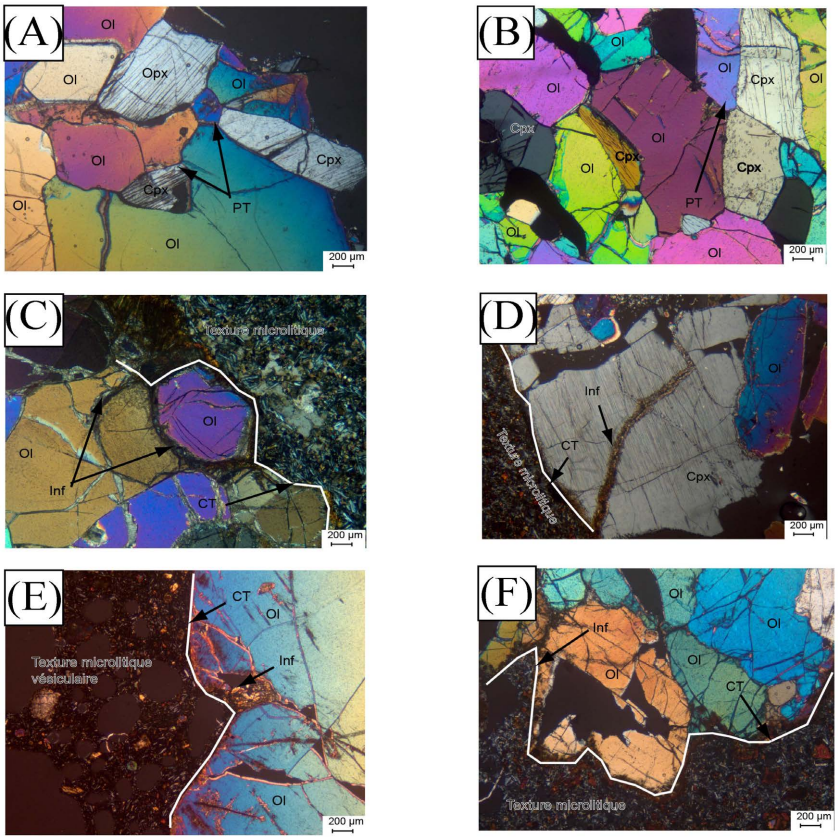

Figure 6. Analyzed polarized light micrographs of protogranular textures in spinel lherzolitic xenoliths showing triple points (A and B) and their contact with host lava. (A): Automorphic fractured olivines with rectilinear edges, showing triple points (PT) between them or with pyroxenes. (B): Olivines and strongly fractured, straight-edged, automorphic pyroxenes showing triple points (PT). (C): Protogranular-textured xenolith in contact with microlitic-textured basanite. At the contact with the lava, fractures and joints between minerals are filled by basaltic seepage (Inf). (D): Protogranular xenolith in contact with microlitic basanite. At the contact with the lava, a large pyroxene mineral shows fractures filled by basaltic infiltration (Inf). (E): Protogranular-textured xenolith in contact with microlitic-textured vesicular scoria. At the contact with the lava, fractures and joints between olivine minerals are filled by basaltic infiltration (Inf). (F): Protogranular-textured xenolith in contact with microlitic-textured basanite, showing basaltic infiltration (Inf) at the contact with lava. Legend: Ol = Olivine; Cpx = Clinopyroxene; Opx = Orthopyroxene; PT = Triple point; CT = Contact; Inf = Basaltic infiltration.

Spinels are generally small along the shorter axis (0.1 to 3 mm). They are rectangular (Figure 7(A)-(D)), polylobed, elongated Figure 7(F), Figure 8(D)-(F) or amoeboid (Figure 7(E) and Figure 7(F), Figure 8(A)-(C)). Some are interstitial, while others are grouped in diverticulate aggregates or small grains aligned between olivine and pyroxene crystals or embedded in other mineral phases (Figure 7(A), Figure 7(B), and Figure 7(D)). Spinels, closely associated with pyroxenes and olivines, take on different forms, reflecting their primary or early spinel nature in the xenoliths studied.

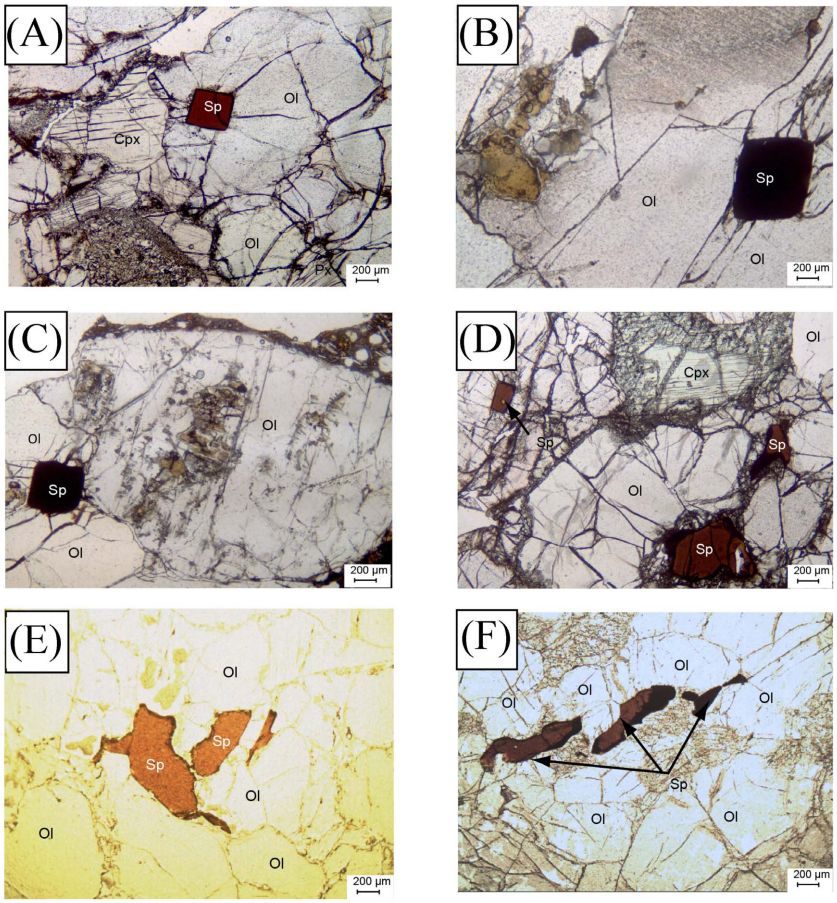

Figure 7. Analyzed polarized light micrographs of protogranular-textured spinel lherzolitic xenoliths illustrate the arrangement of spinels. (A): Rectangular spinel embedded in a large, highly fractured olivine crystal and in contact with a clinopyroxene. (B): Rectangular spinel embedded in a large, highly fractured olivine crystal. (C): Rectangular spinel between junctions of olivine crystals. (D): Rectangular spinel embedded in a strongly fractured olivine crystal with polylobate spinels between olivines. (E): Sub-automorphic amoeboid spinels elongated between olivine minerals or along fractures. (F): Spinels are elongated crystals, polylobed vermicules or amoeboids along the rectilinear contours of olivines. Legend: Sp = Spinel; Cpx = Clinopyroxene; Ol = Olivine.

The sharp contact between protogranular spinel lherzolitic xenolith studies and porphyritic microlitic host basanites is generally irregular or rectilinear (Figure 7(C)-(F)). The minerals in xenoliths have fractures that can be filled by magmatic

fluid, creating a glassy film that can act as a contaminant. These fractures, accompanied by intergranular sliding, are evidence of the interaction between host basalts and mantle xenoliths.

Some olivines have sharp, curved, polygonal contours Figure 8(A) and Figure 8(B). Other olivines, often severely fractured during mobilization, show intergranular slippage or corrosive action when in contact with host lavas. The fractured olivine can also be penetrated by magmatic juices, which may act as basaltic contamination. Recrystallization is nonexistent, and some olivines seem to be affected by the host basalt, which explains their primary nature. In any case, the olivines are not transformed and remain in equilibrium with the host lava. Their intense fracturing results from their re-mobilization in the host lava.

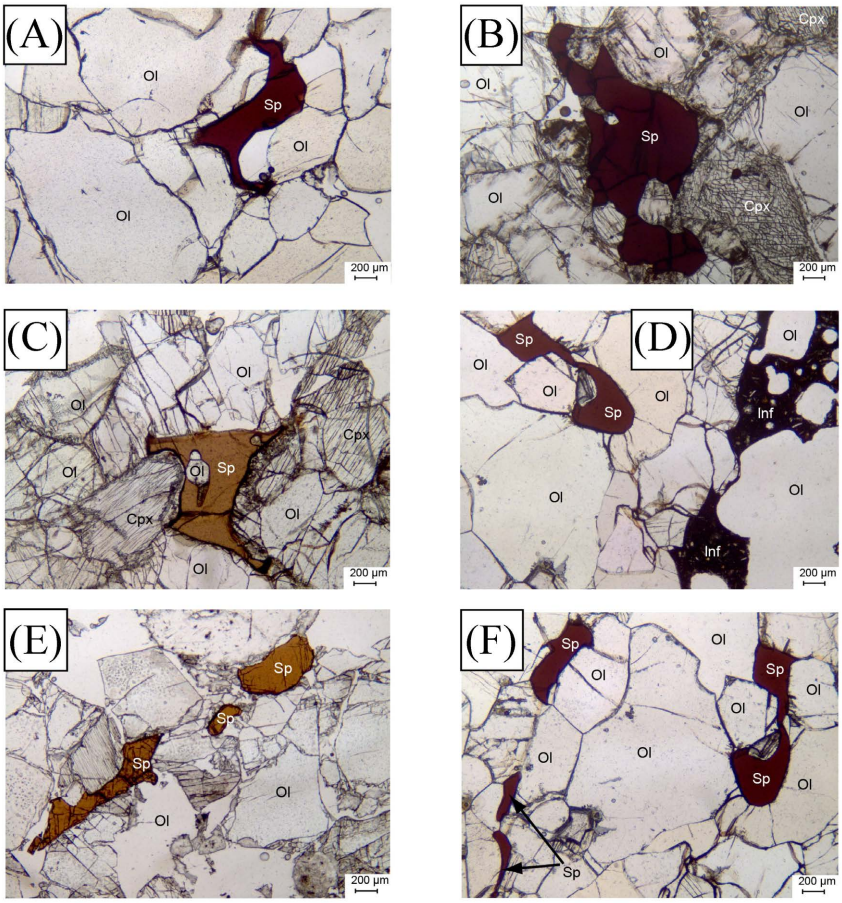

Figure 8. Analyzed polarized light micrographs of protogranular-textured spinel lherzolitic xenoliths illustrating spinel arrangement. (A): Polylobed amoeboid xenomorphic spinel associated with olivines. (B): Polylobed amoeboid xenomorphic spinel associated with olivines and pyroxenes. (C): Polylobed xenomorphic spinel with embedded olivine microcrystals associated with pyroxenes and olivines. (D): Polylobed amoeboid xenomorphic spinel associated with olivines and basaltic infiltrations (Inf). (E): Alignment of elongated amoeboid sub-automorphic spinels between strongly fractured olivine minerals. (F): Alignment of rectangular, needle-like, or amoeboid sub-automorphic spinels between olivine minerals.Legend: Sp = Spinel; Cpx = Clinopyroxene; Ol = Olivine; Inf = Basaltic infiltration.

The modal compositions of the peridotite samples studied show the predominance of olivines (69% - 73%), followed by pyroxenes (6% - 25%) and spinel (0.17% - 3.5%).

These proportions place the xenoliths in the field of Harzburgites, Dunites, and Lherzolites (**Figure 9(A)**) and are comparable to xenoliths from the sub-oceanic mantle (**Figure 9(B)**) in an active margin context (**Figure 9(C)**).

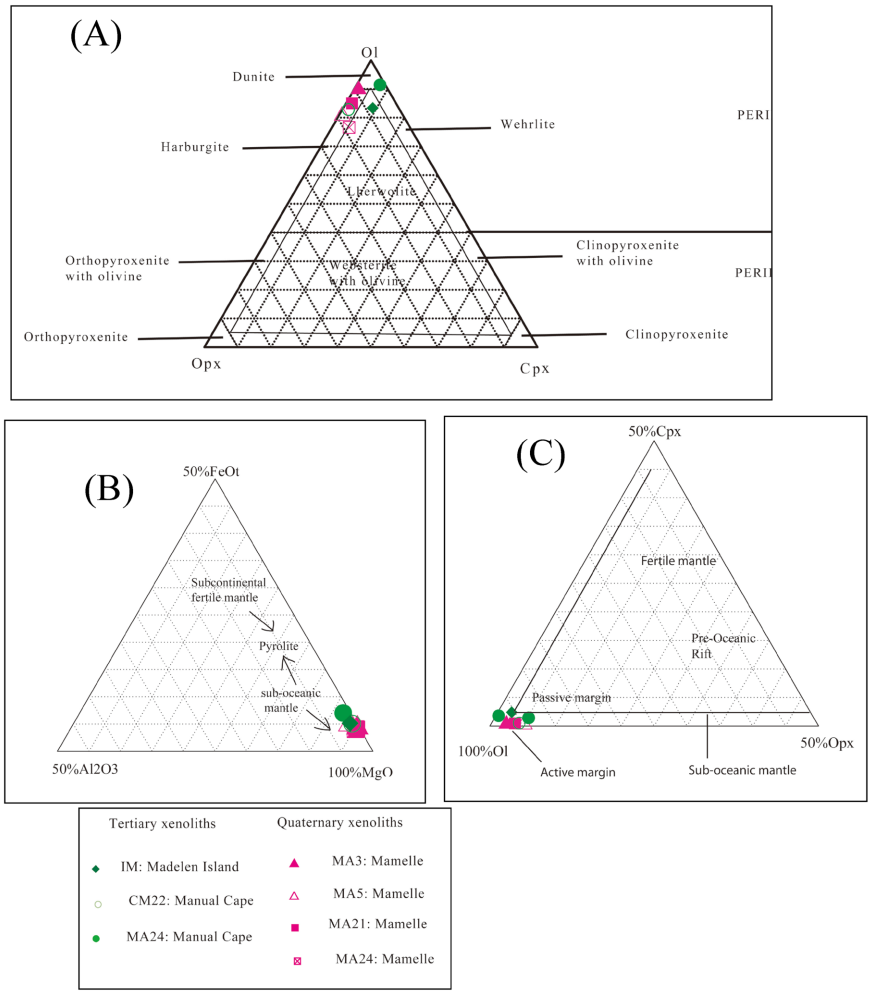

Figure 9. Position of spinel lherzolitic xenoliths in diagrams: (A) = Ol-Cpx-Opx [22]-[24]. (B) = 50% Al_2O_3-50% FeOt-100% Ol [25]. (C) = Ol-50% Cpx-50% Opx [25]. Ol = Olivine; Cpx = Clinopyroxenes; Opx = Orthopyroxenes.

3.2. Chemical Composition of the Mineral Phases of Spinel Lherzolitic Xenoliths

Olivine, orthopyroxenes, and clinopyroxenes form the mineral paragenesis of spinel lherzolitic xenoliths, completed by an aluminous phase, the spinel. The compositions of these mineral phases in the spinel lherzolitic are given in **Tables 1-7**.

3.2.1. Olivines

The Fo content (Fo = Mg/(Mg + FeT)*100) ranges from 89.1 to 91.8 in olivines

from Mamelle xenoliths, 90.3 to 91.8 in olivines from Madelen Island, and 75.9 to 92.4 in olivines from Manual Cape xenoliths (Table 1, Table 2). These high Fo contents, combined with the absence of olivine zonation, are characteristic of peridotite xenoliths found in alkaline basalts worldwide. Globally, these Fo olivine contents are significantly higher than the range estimated for the primitive mantle (88.7 - 90.1), as noted in [26]. The Fo contents of olivines in the studied xenoliths consistently remain higher than those of olivines in the host alkaline basalts (Fo 60 - 91.5) [14].

Table 1. Olivine composition in xenoliths from Quaternary lavas (Mamelle).

		SiO_2	Al_2O_3	TiO_2	Cr_2O_3	FeOt	MnO	MgO	CaO	Na_2O	K_2O	NiO	Total	Fo
Mamelle	MA3	40.36	0.01	0.02	0.03	8.60	0.06	49.61	0.09	0.02	0.00	0.37	99.16	91.15
	MA3	40.63	0.00	0.00	0.00	8.52	0.17	49.48	0.09	0.00	0.00	0.40	99.29	91.20
	MA3	40.92	0.02	0.00	0.00	8.39	0.11	50.71	0.05	0.00	0.02	0.43	100.65	91.51
	MA3	41.56	0.00	0.00	0.00	8.50	0.11	49.42	0.08	0.00	0.00	0.35	100.03	91.20
	MA3	40.67	0.03	0.06	0.04	8.28	0.12	49.98	0.06	0.01	0.00	0.35	99.60	91.52
	MA3	41.22	0.03	0.00	0.01	8.13	0.13	49.75	0.11	0.04	0.01	0.39	99.82	91.59
	MA3	41.16	0.02	0.02	0.03	9.32	0.19	49.52	0.05	0.00	0.06	0.35	100.74	90.47
	MA3	40.68	0.03	0.03	0.00	8.62	0.10	49.90	0.10	0.01	0.01	0.41	99.89	91.18
	MA3	40.66	0.03	0.08	0.00	8.71	0.11	50.13	0.04	0.00	0.02	0.36	100.15	91.10
	MA3	41.48	0.01	0.00	0.02	8.53	0.19	49.78	0.05	0.02	0.00	0.42	100.49	91.23
	MA3	40.93	0.00	0.00	0.09	8.37	0.11	50.13	0.02	0.00	0.03	0.41	100.10	91.46
	MA5	40.59	0.01	0.00	0.04	8.61	0.10	49.67	0.07	0.00	0.00	0.38	99.49	91.12
	MA5	39.88	0.03	0.00	0.00	8.69	0.12	49.92	0.08	0.01	0.02	0.36	99.11	91.13
	MA5	40.98	0.03	0.04	0.02	8.85	0.10	49.73	0.05	0.02	0.00	0.31	100.13	90.95
	MA5	41.65	0.00	0.06	0.00	8.73	0.11	49.62	0.07	0.02	0.00	0.31	100.58	91.01
	MA5	41.22	0.00	0.00	0.01	8.49	0.13	50.35	0.09	0.01	0.00	0.33	100.65	91.36
	MA5	40.56	0.02	0.00	0.02	8.39	0.10	51.33	0.10	0.05	0.01	0.32	100.91	91.59
	MA5	40.44	0.02	0.02	0.00	8.52	0.13	49.80	0.09	0.00	0.00	0.30	99.34	91.25
	MA5	40.90	0.00	0.02	0.01	8.50	0.18	49.84	0.09	0.01	0.00	0.30	99.86	91.25
	MA5	41.16	0.00	0.00	0.01	8.52	0.11	50.00	0.07	0.02	0.00	0.29	100.19	91.29
	MA5	40.78	0.04	0.00	0.00	8.62	0.13	50.01	0.08	0.00	0.01	0.31	99.98	91.18
	MA5	41.25	0.00	0.01	0.09	8.67	0.10	50.01	0.07	0.05	0.02	0.28	100.55	91.13
	MA5	41.21	0.02	0.04	0.05	8.55	0.09	50.13	0.09	0.00	0.00	0.35	100.54	91.29
	MA5	40.66	0.00	0.05	0.03	8.66	0.12	49.95	0.07	0.00	0.00	0.36	99.91	91.14
	MA5	40.66	0.00	0.02	0.00	8.44	0.15	50.18	0.06	0.00	0.00	0.32	99.83	91.40
	MA5	40.81	0.03	0.00	0.00	8.70	0.11	50.10	0.08	0.01	0.00	0.27	100.13	91.14
	MA5	41.40	0.00	0.03	0.00	8.36	0.11	49.55	0.09	0.00	0.02	0.29	99.85	91.37
	MA20	41.48	0.00	0.01	0.00	8.66	0.09	50.61	0.03	0.02	0.04	0.29	101.23	91.26

Continued

Mamelle	MA20	41.40	0.00	0.01	0.03	8.70	0.12	50.69	0.05	0.00	0.00	0.31	101.32	91.23
	MA20	41.22	0.00	0.00	0.03	8.60	0.16	50.71	0.04	0.00	0.01	0.28	101.05	91.30
	MA20	40.75	0.02	0.00	0.00	8.35	0.18	49.96	0.01	0.02	0.00	0.31	99.60	91.42
	MA21	41.52	0.01	0.00	0.00	8.54	0.13	49.97	0.08	0.01	0.02	0.28	100.55	91.25
	MA21	41.15	0.02	0.00	0.01	8.25	0.12	50.57	0.04	0.01	0.00	0.32	100.47	91.62
	MA21	41.31	0.02	0.03	0.02	8.31	0.12	50.88	0.06	0.00	0.00	0.34	101.09	91.63
	MA21	41.19	0.01	0.00	0.09	8.19	0.15	50.10	0.08	0.00	0.00	0.29	100.11	91.58
	MA23	41.53	0.00	0.02	0.05	7.97	0.12	50.25	0.07	0.00	0.00	0.28	100.28	91.81
	MA23	41.09	0.04	0.02	0.06	8.25	0.11	50.05	0.10	0.03	0.01	0.31	100.07	91.53
	MA23	41.18	0.01	0.01	0.01	8.14	0.14	50.55	0.07	0.03	0.01	0.31	100.44	91.72
	MA23	40.99	0.01	0.00	0.07	9.00	0.10	49.44	0.08	0.00	0.00	0.29	99.97	90.73
	MA23	40.89	0.00	0.02	0.00	9.14	0.20	49.93	0.19	0.02	0.00	0.32	100.72	90.68
	MA23	40.87	0.01	0.00	0.04	10.41	0.17	48.00	0.23	0.03	0.00	0.22	99.96	89.16
	MA23	40.80	0.00	0.00	0.04	10.55	0.18	48.28	0.13	0.01	0.02	0.28	100.29	89.06

Table 2. Olivine composition in Xenoliths from Tertiary lavas (Cap Manuel and Madelen Island).

		SiO_2	Al_2O_3	TiO_2	Cr_2O_3	FeOt	MnO	MgO	CaO	Na_2O	K_2O	NiO	Total	Fo
Manual Cap	CM24	40.99	0.00	0.04	0.00	8.14	0.14	50.16	0.00	0.03	0.00	0.30	99.80	91.66
	CM24	38.76	0.02	0.03	0.00	21.21	0.43	39.59	0.58	0.02	0.03	0.10	100.76	76.91
	CM24	58.94	0.10	0.00	0.04	5.42	0.19	35.85	0.11	0.00	0.00	0.09	100.74	92.17
	CM24	58.29	0.16	0.06	0.15	5.34	0.19	35.84	0.20	0.05	0.00	0.05	100.33	92.27
	CM24	40.42	0.01	0.00	0.04	10.07	0.15	48.74	0.03	0.02	0.00	0.33	99.79	89.63
	CM24	39.96	0.00	0.04	0.03	11.75	0.22	46.97	0.23	0.00	0.02	0.25	99.46	87.69
	CM22	56.75	2.37	0.01	0.60	5.41	0.19	34.65	0.68	0.05	0.00	0.09	100.80	91.93
	CM22	56.98	2.36	0.02	0.53	5.11	0.13	34.78	0.60	0.05	0.01	0.05	100.62	92.38
	CM22	56.57	2.37	0.01	0.51	5.40	0.14	34.51	0.62	0.03	0.01	0.09	100.27	91.93
	CM22	57.29	2.38	0.00	0.49	5.34	0.18	34.70	0.66	0.08	0.00	0.04	101.16	92.04
	CM22	56.33	2.34	0.04	0.57	5.40	0.14	34.10	0.79	0.04	0.01	0.04	99.80	91.83
	CM2	40.09	0.01	0.00	0.00	12.49	0.32	46.11	0.17	0.03	0.05	0.23	99.51	86.81
	CM2	39.47	0.04	0.00	0.01	14.04	0.29	45.30	0.36	0.00	0.00	0.21	99.72	85.20
	CM2	39.97	0.04	0.00	0.00	13.39	0.41	45.71	0.08	0.01	0.00	0.25	99.87	85.89
	CM2	40.14	0.00	0.00	0.00	13.98	0.31	45.30	0.34	0.01	0.00	0.19	100.28	85.23
	CM2	40.11	0.02	0.00	0.03	12.04	0.36	47.00	0.04	0.02	0.02	0.28	99.92	87.44
	CM2	40.12	0.00	0.00	0.00	11.98	0.35	47.01	0.00	0.04	0.00	0.30	99.81	87.49
	CM2	40.15	0.02	0.00	0.00	12.12	0.37	46.62	0.01	0.00	0.03	0.32	99.64	87.30
	CM2	39.99	0.00	0.04	0.01	12.36	0.28	46.53	0.11	0.00	0.00	0.33	99.65	87.02
	CM2	39.69	0.00	0.05	0.00	11.86	0.35	47.01	0.01	0.03	0.00	0.29	99.29	87.60

Continued

Manual Cap	CM2	39.54	0.01	0.01	0.00	11.99	0.33	46.96	0.15	0.02	0.00	0.29	99.29	87.47
	CM2	40.02	0.00	0.03	0.01	12.10	0.32	47.03	0.03	0.00	0.00	0.35	99.89	87.37
	CM2	39.59	0.01	0.09	0.00	12.75	0.29	46.36	0.13	0.02	0.00	0.27	99.51	86.64
	CM2	40.21	0.00	0.00	0.00	11.91	0.36	47.07	0.01	0.18	0.01	0.32	100.09	87.57
	CM2	39.80	0.00	0.07	0.05	11.80	0.32	46.45	0.12	0.01	0.00	0.34	98.97	87.54
	CM2	38.30	0.05	0.00	0.02	20.30	0.40	39.66	0.41	0.07	0.00	0.14	99.35	77.68
	CM2	37.52	0.05	0.00	0.04	21.26	0.50	39.33	0.53	0.00	0.00	0.14	99.37	76.72
	CM2	38.01	0.05	0.04	0.00	21.91	0.48	38.65	0.67	0.03	0.01	0.19	100.03	75.86
Madelen Island	IM1	40.36	0.00	0.00	0.02	9.23	0.10	49.52	0.10	0.00	0.03	0.35	99.72	90.52
	IM1	40.16	0.01	0.01	0.04	8.92	0.15	49.08	0.05	0.02	0.04	0.37	98.86	90.74
	IM1	40.58	0.03	0.00	0.00	9.09	0.13	49.68	0.06	0.00	0.00	0.35	99.92	90.70
	IM1	39.86	0.03	0.02	0.04	9.30	0.09	49.00	0.13	0.00	0.01	0.37	98.86	90.38
	IM1	40.80	0.00	0.00	0.10	9.27	0.16	49.35	0.17	0.01	0.00	0.38	100.25	90.44
	IM1	40.66	0.00	0.02	0.05	9.03	0.15	49.59	0.15	0.00	0.03	0.44	100.12	90.72
	IM1	40.55	0.01	0.00	0.02	9.14	0.13	49.69	0.15	0.00	0.01	0.39	100.09	90.65
	IM1	40.97	0.02	0.00	0.08	9.24	0.13	49.57	0.12	0.00	0.04	0.29	100.47	90.54
	IM1	41.04	0.01	0.00	0.01	9.51	0.12	49.61	0.13	0.01	0.00	0.32	100.76	90.31
	IM1	41.26	0.00	0.00	0.03	8.80	0.11	49.59	0.22	0.00	0.02	0.23	100.26	90.95
	IM1	57.61	0.65	0.11	0.41	5.64	0.14	33.14	1.35	0.24	0.16	0.06	99.52	91.29

The NiO content of olivines ranges from 0.151% to 0.425% for olivines from Mamelle xenoliths, 0.057% to 0.442% for those from Madelen Island, and 0.039% to 0.351% for those from Manual Cape. These NiO contents fall within the normal range (0.28% to 0.30% by weight) of olivines from the primitive mantle (PM) [26].

Correlations between NiO content and Mg# (**Figure 10**) show a positive trend from Cape Manuel to Mamelle spinel lherzolitic xenoliths. These variations are similar to the Lherzolite xenolith type [21].

CaO contents remain globally low, ranging from 0.0129% to 0.478% in the olivines of the Mamelle xenoliths, from 0% to 0.79% for the Manual Cape olivines, and 0.048% to 1.352% for those of Madelen Island.

Chromium content oscillates between 0 and 0.094 in the olivines of the Mamelle xenoliths, 0 to 0.603 in the olivines of Manual Cape, and 0 to 0.406 in those of Madelen Island.

These variations in the chemical elements Fo, NiO and CaO are compatible with a mantle origin of the xenoliths studied.

3.2.2. Pyroxenes

The pyroxenes in the xenoliths studied are augite or diopside for the clinopyroxenes ($Wo_{37.16\text{-}51.27}$-$En_{37.02\text{-}65.52}$-$Fs_{3.2\text{-}11.72}$) and clinoenstatites for the orthopyroxenes ($Wo_{1.31\text{-}1.53}$-$En_{90.08\text{-}90.54}$-$Fs_{8.01\text{-}8.55}$) in the Morimoto classification diagram [27] (**Figure 11**).

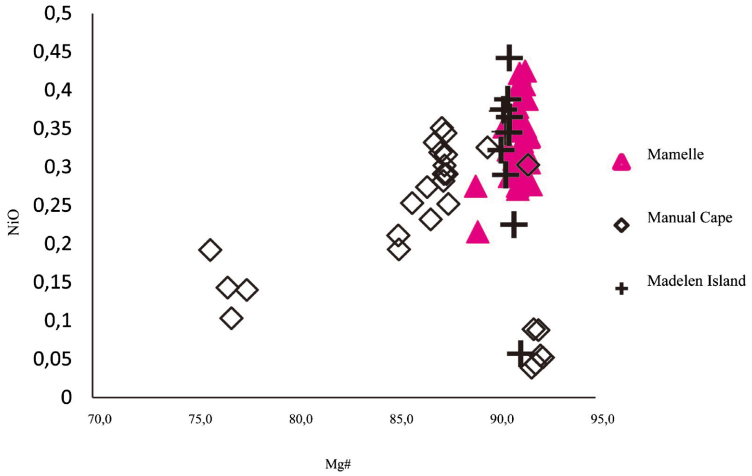

Figure 10. Variations in NiO content vs. Mg# in olivines from spinel lherzolitic xenoliths in Mamelle Quaternary lavas and Manual Cape and Madelen Island from spinel lherzolitic xenoliths in Tertiary lava of the Senegal Cape Verde Peninsula.

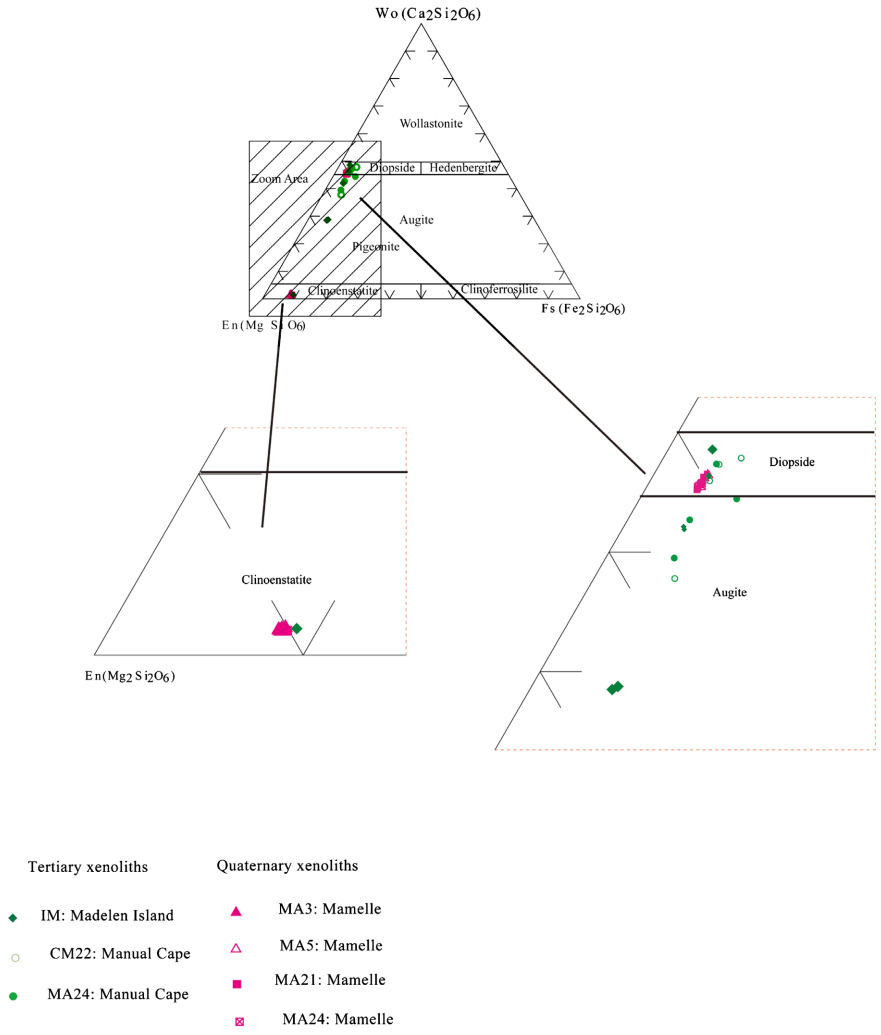

Figure 11. Projection of pyroxene compositions of spinel lherzolitic xenoliths in Tertiary and Quaternary lavas in the Morimoto diagram [27].

1) Clinopyroxenes

Clinopyroxenes in quaternary xenoliths (Mamelle) (Table 3) have Cr_2O_3 contents ranging from 0.82 to 1.27%, TiO_2 from 0.00 to 0.21% and Al_2O_3 from 1.21 to 4.69%.

Clinopyroxenes in tertiary lava xenoliths (Table 4) from Manual Cape have higher Cr_2O_3 (0.4% - 4.66%), TiO_2 (0.06% - 2.22%), and Al_2O_3 (0.5% - 7.92%) contents than those from Madelen Island, where these values are 0.434% - 4.656%, 0.00% - 0.217% and 0.579% - 7.92% respectively. Na_2O contents remain comparable, ranging from 0.49% to 2.24% for clinopyroxenes from Manual Cape xenoliths, compared with 0.47% to 2.286% for xenoliths from Madelen Island.

Table 3. Clinopyroxene composition in xenoliths from Quaternary lavas.

		SiO_2	Al_2O_3	TiO_2	Cr_2O_3	Fe_2O_3	FeO	MnO	MgO	CaO	Na_2O	K_2O	NiO	Tot. ox. calc	Mg#
Mamelle	MA23	53.01	4.59	0.17	1.22	0.00	2.14	0.07	16.24	21.21	1.04	0.00	0.02	99.70	93.10
	MA23	52.67	4.49	0.17	1.07	0.09	2.01	0.07	16.39	21.13	1.02	0.00	0.03	99.14	93.39
	MA23	53.19	4.54	0.10	1.11	0.20	2.10	0.05	16.47	21.22	1.06	0.01	0.05	100.10	92.87
	MA5	53.20	4.60	0.17	0.93	0.13	2.16	0.04	16.50	21.22	1.07	0.00	0.00	100.03	92.89
	MA5	52.56	4.50	0.12	1.07	1.44	0.89	0.08	16.49	21.20	1.15	0.02	0.04	99.56	93.11
	MA5	53.33	4.64	0.21	1.01	0.26	2.11	0.07	16.40	21.38	1.10	0.01	0.04	100.55	92.62
	MA5	53.04	4.54	0.17	1.06	1.18	1.15	0.08	16.42	21.44	1.20	0.01	0.03	100.32	92.93
	MA5	53.27	4.69	0.15	1.13	0.39	1.80	0.09	16.64	21.13	1.10	0.03	0.03	100.43	93.30
	MA3	52.59	4.61	0.20	1.03	1.54	0.81	0.08	16.64	21.24	1.14	0.01	0.00	99.88	93.15
	MA20	54.78	2.51	0.02	1.10	0.00	2.34	0.04	16.72	21.30	1.08	0.00	0.06	99.96	92.69
	MA20	54.69	2.59	0.01	1.14	0.41	1.99	0.09	16.72	21.87	1.17	0.01	0.02	100.72	93.72
	MA20	54.50	2.59	0.00	1.25	0.08	2.16	0.06	16.69	21.48	1.21	0.02	0.03	100.06	93.26
	MA20	54.70	2.66	0.01	1.23	0.35	2.27	0.09	16.65	21.79	1.18	0.00	0.00	100.92	92.90
	MA20	55.23	1.22	0.07	0.82	0.05	3.09	0.08	20.35	18.90	0.53	0.00	0.00	100.33	92.12
	MA20	55.24	1.21	0.04	0.82	0.34	2.84	0.13	20.77	18.58	0.47	0.02	0.02	100.50	92.86
	MA20	54.33	2.41	0.01	1.01	0.36	2.06	0.07	16.63	21.72	1.16	0.00	0.02	99.77	93.55
	MA21	53.33	3.61	0.14	1.28	0.95	1.37	0.07	17.19	21.76	0.83	0.01	0.04	100.58	95.74
	MA21	53.51	3.67	0.17	1.21	0.00	2.30	0.10	16.92	21.20	0.74	0.02	0.07	99.92	92.87
	MA21	53.50	3.55	0.11	1.20	0.36	1.87	0.08	17.20	21.77	0.74	0.02	0.06	100.47	94.28
	MA21	53.91	3.43	0.05	1.21	0.00	2.29	0.08	17.31	21.76	0.72	0.00	0.04	100.79	93.07
	MA21	53.93	3.65	0.14	1.13	0.00	2.12	0.13	17.22	21.71	0.73	0.01	0.03	100.81	93.50
	MA21	53.86	3.52	0.12	1.20	0.00	2.24	0.09	16.99	21.37	0.70	0.00	0.03	100.11	93.16
	MA21	54.17	3.56	0.18	1.27	0.00	2.22	0.07	17.32	21.35	0.71	0.01	0.05	100.89	93.33
	MA21	53.52	3.68	0.15	1.24	0.00	2.14	0.10	17.16	21.21	0.73	0.00	0.01	99.94	93.43
	MA21	53.57	3.52	0.08	1.24	0.00	2.18	0.07	16.97	21.07	0.71	0.01	0.04	99.46	93.29
	MA21	53.34	3.60	0.11	1.21	0.00	2.16	0.03	17.13	21.34	0.73	0.01	0.03	99.70	93.43
	MA21	53.65	3.55	0.14	1.17	0.00	2.10	0.14	17.17	21.49	0.74	0.01	0.02	100.18	93.61
	MA21	53.07	3.59	0.11	1.16	0.39	1.96	0.04	17.09	21.56	0.74	0.00	0.03	99.75	94.00

Table 4. Clinopyroxene composition in Xenoliths from Tertiary lavas (Manual Cape and Madelen Island).

		SiO_2	Al_2O_3	TiO_2	Cr_2O_3	Fe_2O_3	FeO	MnO	MgO	CaO	Na_2O	K_2O	NiO	Tot. ox. calc	Mg#
Manual Cape	CM22	54.49	1.29	0.44	1.48	0.36	3.12	0.15	19.47	18.18	0.89	0.04	0.04	99.96	91.77
	CM22	53.46	3.24	0.06	1.27	0.03	2.44	0.10	16.58	21.31	0.99	0.00	0.01	99.48	92.39
	CM22	53.21	2.65	0.50	1.37	0.12	2.44	0.09	16.58	22.57	0.64	0.02	0.06	100.23	92.38
	CM22	51.40	4.09	0.89	1.22	1.47	2.05	0.05	15.78	22.58	0.66	0.00	0.03	100.22	93.25
	CM2	53.52	1.55	0.58	1.67	0.62	2.40	0.06	16.56	22.65	0.75	0.01	0.02	100.37	90.88
	CM2	54.17	3.48	0.65	1.30	0.00	3.21	0.05	15.24	23.25	0.70	0.00	0.03	102.07	89.42
	CM2	53.22	1.85	0.68	1.32	1.56	1.94	0.06	16.56	22.85	0.74	0.01	0.03	100.81	89.76
	CM2	50.80	6.71	1.87	0.58	0.00	4.45	0.07	13.39	23.12	0.49	0.01	0.00	101.48	84.35
	CM2	51.47	3.20	0.68	1.24	2.04	2.62	0.09	15.44	23.10	0.49	0.00	0.08	100.44	86.09
	CM2	45.67	7.92	2.22	0.43	4.33	2.79	0.09	12.02	23.18	0.56	0.01	0.03	99.24	76.22
	CM2	54.48	0.82	0.31	1.62	0.85	1.91	0.11	17.35	21.83	0.97	0.00	0.02	100.26	92.04
	CM2	53.07	1.54	0.45	1.26	1.81	1.46	0.00	16.75	22.81	0.71	0.01	0.00	99.87	90.65
	CM2	52.72	2.01	0.50	1.11	1.72	1.68	0.14	16.62	22.51	0.67	0.03	0.03	99.74	90.24
	CM2	54.74	0.83	0.32	1.84	0.35	2.68	0.15	17.06	21.10	1.17	0.00	0.05	100.28	91.01
	CM2	49.25	5.14	1.81	0.85	2.34	2.53	0.08	14.30	23.14	0.59	0.02	0.02	100.06	84.59
	CM2	54.69	1.03	0.39	1.40	0.00	2.74	0.10	17.05	22.39	0.71	0.01	0.02	100.53	91.72
	CM24	54.96	0.91	0.22	2.42	1.12	1.60	0.13	17.98	20.25	1.32	0.02	0.02	100.96	92.50
	CM24	53.06	1.99	0.77	1.23	1.07	1.50	0.08	16.84	22.85	0.67	0.03	0.09	100.18	92.40
	CM24	52.13	2.57	0.40	1.47	1.55	2.77	0.09	16.54	21.10	0.67	0.05	0.06	99.41	87.62
	CM24	54.73	0.58	0.07	4.66	0.59	2.14	0.08	17.33	17.14	2.24	0.01	0.00	99.56	92.06
Madelen Island	IM1	53.85	5.01	0.35	0.89	3.99	0.00	0.03	21.04	12.97	2.29	1.21	0.11	101.72	91.29
	IM1	53.84	2.54	0.23	1.36	0.38	1.57	0.08	16.86	23.64	0.54	0.02	0.01	101.06	94.06
	IM1	52.28	1.29	0.10	0.82	4.50	0.00	0.10	25.42	15.39	0.83	0.26	0.08	101.05	91.83
	IM1	55.62	0.80	0.20	1.07	0.00	2.64	0.06	18.70	20.48	0.86	0.11	0.05	100.58	92.68
	IM1	53.35	1.88	0.28	1.57	2.11	0.51	0.08	17.00	22.11	0.92	0.18	0.04	100.01	92.65
	IM1	52.60	3.03	0.28	1.34	3.02	0.00	0.10	18.90	20.54	0.76	0.04	0.02	100.63	92.50

Al^{IV}/Al^{VI} ratios, ranging from 0.16 to 19.32, are comparable to those of clinopyroxenes from subcontinental upper mantle peridotites, GERM see [26].

The Mg# differentiation index ($Mg^{2+}/Mg^{2+} + Fe^{2+} + Fe^{3+} + Mn^{2+}$) is relatively lower in the clinopyroxenes of the Tertiary xenoliths of Manual Cap (82.8 - 89.7), slightly higher in those of Madelen Island (91.5 - 93.7) and around 91.6 to 93.2 in the clinopyroxenes of the Quaternary xenoliths of Mamelle. Na_2O shows a positive correlation with Mg# (**Figure 12(A)**), while Al_2O_3 and TiO_2 contents show a negative correlation (**Figure 12(B)** and **Figure 12(C)**). These variations are comparable to those observed in Lherzolites. Variations in CaO, Al_2O_3, Cr_2O_3, and NiO contents indicate a less depleted, more refractory character [28]. Ti and Na variations in clinopyroxenes display no clear trend towards simultaneously decreasing

concentrations of both oxides.

2) Orthopyroxenes

The highly magnesian orthopyroxenes have Mg# (Mg^{2+}/Mg^{2+} + Fe^{2+} total) + Mn^{2+} ratios that vary between 90.8 and 91.68. Al_2O_3 contents range from 3.52% to 3.786%, with Cr_2O_3 (0.468% - 0.624%), TiO_2 (0.01% - 0.105%), and Na_2O (0.022% - 0.098%) (Table 5). CaO contents remain low between 0.679 and 0.781%. The variations content of Al_2O_3 and Cr_2O_3 may be attributable to the partial melting process. For almost constant Mg# values, Na_2O, Al_2O_3 and TiO_2 contents show significant variation ranges (Figure 12(D)~(F)) comparable to those observed in Lherzolite xenoliths [28]. Variations in other incompatible (CaO, Na_2O, K_2O) and compatible (Cr_2O_3 and NiO) elements during melting confirm the residual nature of xenoliths resulting from the partial melting process [28].

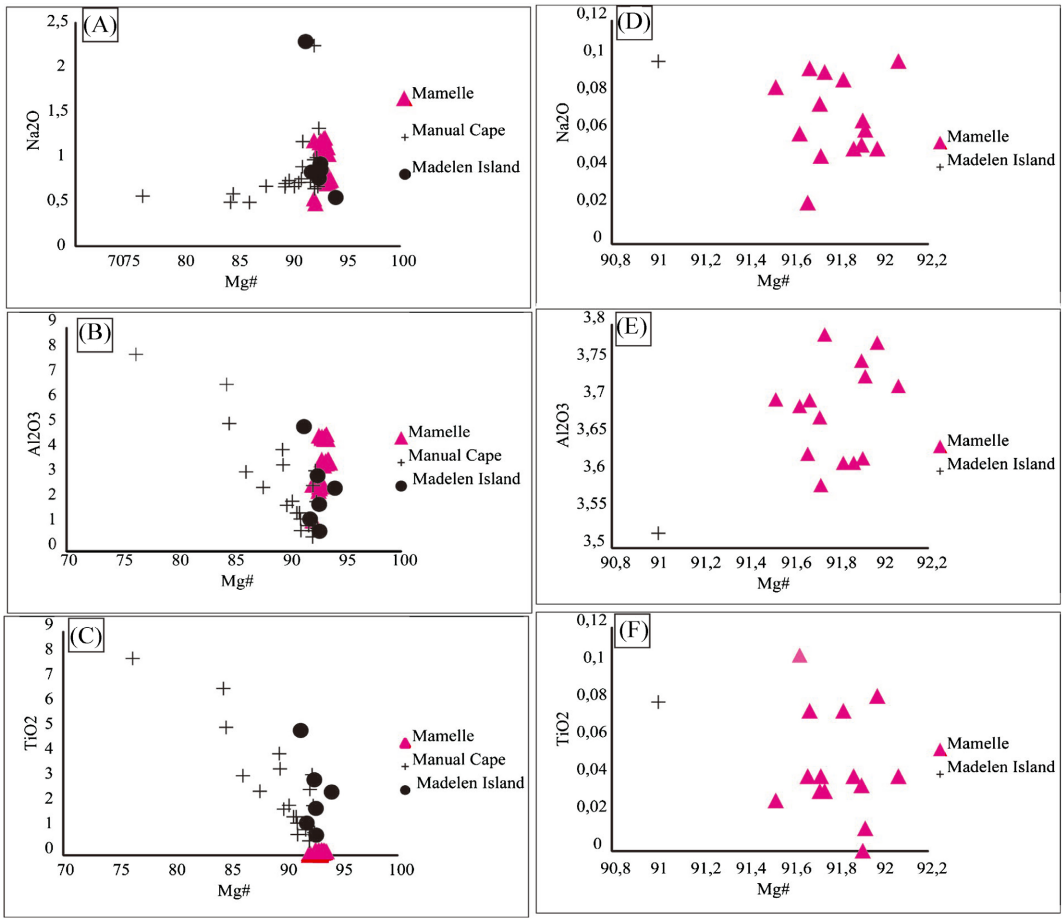

Figure 12. Na_2O (A), Al_2O_3 (B) and TiO_2 (C) versus Mg# in clinopyroxenes of spinel lherzolitic xenoliths alkaline lava of the Senegal Cape Verde peninsula Na_2O (D), Al_2O_3 (E) and TiO_2 (F) versus Mg# in orthopyroxenes of spinel lherzolitic xenoliths in alkaline lava of the Senegal Cape Verde peninsula.

Table 5. Orthopyroxene composition in xenoliths from Quaternary (Mamelle) and tertiary (Madelen Island) lavas.

		SiO_2	Al_2O_3	TiO_2	Cr_2O_3	Fe_2O_3	FeO	MnO	MgO	CaO	Na_2O	K_2O	NiO	Tot. ox. calc	Mg#
Mamelle	MA3	56.11	3.73	0.01	0.55	0.00	5.27	0.14	33.63	0.71	0.06	0.01	0.12	100.34	91.92

Continued

Mamelle	MA3	56.14	3.79	0.03	0.57	0.12	5.31	0.16	33.82	0.68	0.09	0.00	0.10	100.81	91.74
	MA3	55.69	3.62	0.00	0.62	0.29	5.02	0.11	33.65	0.74	0.07	0.04	0.12	99.97	91.91
	EP MA3	55.98	3.58	0.04	0.47	0.00	5.38	0.08	33.49	0.76	0.05	0.00	0.06	99.89	91.72
	EP MA3	55.72	3.63	0.04	0.60	0.23	5.24	0.13	33.70	0.78	0.02	0.00	0.12	100.20	91.67
	EP MA3	55.84	3.69	0.11	0.58	0.00	5.43	0.09	33.28	0.78	0.06	0.00	0.12	99.98	91.63
	EP MA3	55.56	3.61	0.04	0.59	0.15	5.15	0.16	33.62	0.69	0.05	0.00	0.12	99.74	91.87
	EP MA3	55.64	3.70	0.08	0.60	0.10	5.34	0.12	33.44	0.71	0.09	0.04	0.07	99.91	91.68
	MA23	55.30	3.70	0.03	0.57	1.06	4.63	0.15	33.63	0.70	0.08	0.02	0.09	99.94	91.53
	MA5	55.28	3.75	0.04	0.61	1.07	4.33	0.13	33.85	0.76	0.05	0.02	0.05	99.95	91.90
	MA5	55.26	3.72	0.04	0.56	1.27	4.05	0.12	33.92	0.75	0.10	0.00	0.06	99.84	92.07
	MA5	55.34	3.61	0.08	0.57	1.45	4.12	0.11	33.98	0.73	0.09	0.00	0.10	100.18	91.82
	MA5	56.09	3.68	0.03	0.54	0.00	5.40	0.10	33.58	0.71	0.08	0.00	0.06	100.25	91.72
	MA5	56.33	3.78	0.08	0.54	0.00	5.26	0.13	33.80	0.75	0.05	0.04	0.07	100.82	91.97
Madelen Island	IM1	56.10	3.52	0.08	0.57	0.08	5.84	0.08	33.49	0.76	0.10	0.01	0.07	100.71	91.01

3.2.3. Spinels

The spinels studied in the spinel lherzolitic xenoliths are rich in alumina, chromium, iron (both ferrous and ferric), magnesium, and less abundantly in nickel and titanium (**Table 6** and **Table 7**). The Mg# ratio (= 100 Mg/[Mg + Fe^{2+} + Fe^{3+}]) ranges from 62.99% to 84.24%, while the Cr# ratio (= 100 Cr/[Cr + Al]) varies from 18.05% to 44.3%. These ratios are very similar to the spinels from lherzolites defined by Arai [29]. However, they are higher than the spinels from Cameroon line peridotite xenoliths, which are aluminous with Mg# values between 74% and 78% for lower Cr# values (8.85% - 14.10%) [30].

The values of Fe^{2+}/Fe^{2+} + Mg^{2+} ratios (0.1378 - 0.3306) and $Fe^{3+}/(Fe^{3+}$ + Al + Cr) (0.0027 - 0.0348) show wide ranges of variation in xenolith spinels.

Lherzolitic spinels in xenoliths from Tertiary volcanism (Manual Cape and Madelen Island) are richer in Fe_2O_3 (0 - 7.39%), FeO (10.15% - 47.42%), TiO_2 (0.16% - 22.02%), MgO (1.90% - 18.156%), and NiO (0.0013% - 0.267%) than spinels from Quaternary volcanic peridotites (Mamelle), which have relatively higher Cr_2O_3 (21% - 33.68%) and relatively lower Fe_2O_3 (0.4% - 1.82%), FeO (9% - 10.94%), TiO_2 (0.05% - 0.16%), MgO (16.84% - 19.52%) and NiO (0.14% - 0.34%) values. These values are comparable to those of the lherzolites defined by Arai [29].

The variations in these elements, as well as in Cr#, and the absence of inclusion in other mineral phases, support a primary and residual nature of the spinels, which likely originated in the mantle [28] [31] [32].

Al vs. Cr and YFe ($Fe^{3+}/(+Cr^{3+}$ + Al^{3+} + Fe^{3+}) vs. XFe (Fe^{2+}/Fe^{2+} + Mg^{2+}) diagrams of spinels show two distinct groups in xenoliths from Quaternary volcan-

ism. **Group 1** is more aluminous and less rich in iron and chromium (MA3 - MA5), while **Group 2** is less aluminous and richer in iron and chromium (MA21 - MA23) (Figure 13 and Figure 14). Spinels from xenoliths in the Tertiary lavas of Manual Cape (CM22 - CM24) and Madelen Island (IM1) have alumina, iron, and chromium characteristics intermediate between these two groups of spinels in the Quaternary xenoliths of Mamelle. However, two spinels show relatively low values for alumina, chromium, and iron.

Table 6. Spinel composition in xenoliths from Quaternary (Mamelle) lavas.

		SiO_2	Al_2O_3	TiO_2	Cr_2O_3	Fe_2O_3	FeO	MnO	MgO	NiO	CaO	Na_2O	K_2O	Tot. rec	Mg#	Cr*100/Cr + Al
Mamelle	MA5	0.04	45.82	0.12	22.30	0.90	9.73	0.14	18.88	0.31	0.00	0.00	0.02	98.26	76.14	24.61
	MA5	0.08	45.51	0.11	22.33	1.43	9.44	0.14	19.12	0.26	0.00	0.04	0.01	98.48	76.07	24.77
	MA5	0.05	46.06	0.11	22.97	1.06	9.62	0.11	19.27	0.31	0.01	0.00	0.00	99.56	76.45	25.05
	MA5	0.05	46.33	0.13	22.16	0.95	9.64	0.12	19.14	0.27	0.00	0.01	0.02	98.82	76.47	24.28
	MA5	0.04	47.08	0.10	22.33	0.65	9.87	0.07	19.27	0.26	0.00	0.05	0.00	99.71	76.67	24.13
	MA5	0.03	45.97	0.14	22.31	0.62	9.70	0.12	18.90	0.31	0.03	0.00	0.02	98.15	76.65	24.54
	MA5	0.04	46.60	0.06	21.12	1.04	9.38	0.14	19.05	0.26	0.02	0.02	0.00	97.72	76.69	23.30
	MA5	0.03	46.39	0.12	21.07	1.14	9.14	0.13	19.17	0.27	0.00	0.00	0.00	97.46	77.07	23.35
	MA5	0.01	45.48	0.15	21.75	1.44	9.27	0.12	19.01	0.27	0.00	0.01	0.00	97.51	76.24	24.29
	MA5	0.07	45.92	0.13	21.99	1.41	9.41	0.07	19.23	0.34	0.00	0.03	0.00	98.59	76.25	24.31
	MA5	0.07	46.39	0.12	21.74	1.24	9.37	0.14	19.30	0.28	0.00	0.01	0.02	98.69	76.63	23.90
	EP MA3	0.05	46.07	0.05	22.61	0.77	9.64	0.16	19.01	0.23	0.01	0.00	0.01	98.61	76.63	24.79
	EP MA3	0.02	46.78	0.14	22.36	0.46	10.09	0.17	18.93	0.29	0.02	0.01	0.01	99.28	76.27	24.28
	EP MA3	0.07	45.70	0.08	22.21	1.35	9.50	0.18	19.02	0.29	0.02	0.02	0.01	98.44	75.99	24.58
	EP MA3	0.03	45.96	0.11	22.66	1.51	9.06	0.17	19.52	0.28	0.02	0.00	0.02	99.32	76.95	24.85
	EP MA3	0.02	46.06	0.12	22.38	0.85	9.71	0.15	18.97	0.24	0.00	0.01	0.00	98.50	76.36	24.57
	EP MA3	0.03	47.18	0.10	22.28	0.78	9.95	0.07	19.27	0.24	0.02	0.03	0.03	99.97	76.33	24.05
	EP MA3	0.07	47.22	0.10	21.70	0.89	9.55	0.11	19.41	0.20	0.03	0.01	0.00	99.29	76.98	23.54
	MA21	0.02	36.64	0.15	33.63	0.85	10.94	0.18	17.56	0.15	0.00	0.03	0.02	100.17	72.79	38.11
	MA21	0.02	36.51	0.16	33.29	1.39	10.05	0.20	18.06	0.16	0.00	0.03	0.00	99.88	74.02	37.96
	MA21	0.07	37.08	0.06	33.68	0.46	10.85	0.19	17.66	0.19	0.00	0.00	0.01	100.26	73.65	37.86
	MA23	0.05	37.05	0.08	32.94	0.90	10.49	0.17	17.77	0.19	0.01	0.01	0.00	99.66	73.72	37.37
	MA23	0.04	36.48	0.10	32.48	1.19	10.60	0.18	17.43	0.14	0.01	0.00	0.00	98.64	72.69	37.39
	MA23	0.03	36.86	0.12	33.01	1.83	9.46	0.18	18.51	0.14	0.05	0.00	0.00	100.18	74.82	37.53
	MA23	0.05	37.39	0.11	32.70	0.42	10.66	0.18	17.65	0.15	0.01	0.01	0.00	99.33	74.04	36.98
	MA23	0.03	34.80	0.13	32.82	1.21	10.72	0.14	16.84	0.16	0.01	0.02	0.01	96.88	71.76	38.75

Table 7. Spinel composition in xenoliths from Tertiary (Manual Cape Madelen Island) lavas.

		SiO_2	Al_2O_3	TiO_2	Cr_2O_3	Fe_2O_3	FeO	MnO	MgO	NiO	CaO	Na_2O	K_2O	Tot. rec	Mg#	Cr*100/Cr + Al
Manual Cape	CM24	0.10	13.54	11.58	27.81	3.70	36.91	0.41	4.17	0.20	0.07	0.02	0.01	98.53	76.14	22.02
	CM24	0.00	4.90	0.65	56.90	7.39	22.52	0.42	6.66	0.02	0.03	0.00	0.02	99.50	76.13	18.06
	CM22	0.24	5.40	2.35	60.26	1.07	18.03	0.36	10.74	0.00	0.02	0.01	0.06	98.55	69.09	24.04
	CM22	0.21	5.79	2.64	57.75	2.70	19.80	0.40	9.84	0.04	0.08	0.07	0.05	99.37	65.19	24.34
	CM22	0.07	1.66	22.02	23.55	0.60	47.42	0.85	1.90	0.06	0.12	0.02	0.00	98.27	84.24	29.47
	CM22	3.76	29.05	0.27	34.46	0.00	14.64	0.17	16.63	0.20	0.10	0.06	0.07	99.40	66.62	44.29
Madelen Island	IM1	0.05	39.72	0.22	28.17	2.26	10.69	0.17	17.94	0.16	0.00	0.03	0.00	99.41	71.53	32.25
	IM1	0.03	40.32	0.26	28.34	1.57	11.10	0.16	17.82	0.16	0.02	0.00	0.00	99.77	71.74	32.05
	IM1	0.03	38.68	0.27	27.70	3.18	13.79	0.20	15.89	0.24	0.00	0.00	0.00	99.98	62.99	32.46
	IM1	0.06	38.38	0.22	28.03	3.23	13.10	0.22	16.24	0.22	0.00	0.04	0.00	99.73	64.39	32.88
	IM1	0.07	39.23	0.25	27.94	2.43	10.15	0.10	18.12	0.27	0.01	0.02	0.00	98.57	72.35	32.33
	IM1	0.07	40.05	0.25	28.09	1.49	11.13	0.08	17.72	0.20	0.00	0.01	0.00	99.10	71.70	31.98
	IM1	0.01	39.61	0.23	28.31	2.45	10.78	0.19	17.87	0.22	0.00	0.01	0.00	99.67	71.05	32.40
	IM1	0.05	39.92	0.16	27.51	2.60	10.19	0.14	18.16	0.22	0.00	0.01	0.00	98.95	72.10	31.61
	IM1	0.05	39.60	0.18	28.34	1.99	10.33	0.15	18.03	0.25	0.00	0.00	0.00	98.92	72.62	32.44

The composition and stability of chromiferous spinels in basic and ultrabasic rocks depend not only on magma composition, temperature, and pressure but also on oxygen fugacity [33] [34]. According to Fisk *et al.* [35], the increase in ferric iron (Fe_2O_3) in chromiferous spinels can be explained by the decrease in temperature under constant oxygen fugacity. On the other hand, experimental studies have shown that Fe^{3+} enrichment can also result from an increase in Fe_2O_3 in the liquid (or magma) linked directly linked to the iron concentration of the liquid (or magma) at constant temperature and oxygen fugacity. Finally, regardless of temperature and composition, the Fe^{3+} content of spinels increases with oxygen fugacity.

In the xenoliths studied, Fe^{3+} enrichment is coupled with an increase in Fe^{2+} and a decrease in Mg^{2+}. Spinels in xenoliths from Tertiary volcanism are richer in Fe_2O_3 (0 to 7.39%) than those in xenoliths from Quaternary volcanism (0.4 to 1.83%). These results are probably due to a higher degree of oxidation in Tertiary xenoliths.

The chemical composition of spinels can determine the origin and formation conditions of the xenoliths studied by Arai [29]. The Quaternary Mamelle and Tertiary Madelen Island spinel lherzolitic xenoliths fall within the olivine-spinel mantle area defined by Arai [29] and are classified as olivine-spinel mantles (OSMA) and continental passive margin peridotites, with a chemical composition close to fertile mantles [29] (**Figure 15**). The degree of melting is estimated to be between 10% and 15% [29]. Cr/Cr + Al ratios in spinels range from 0.1805 to 0.443

in the Mamelle xenoliths and are constant in those from Madelen Island (0.32), for an olivine Fo of 90.5 to 91.5 and 90.3 to 90.7, respectively. These values are comparable to those of oceanic shelf basalt peridotites, oceanic hotspot peridotites, and also the sub-continental fertile peridotites group and those of the island arc of Japan [29].

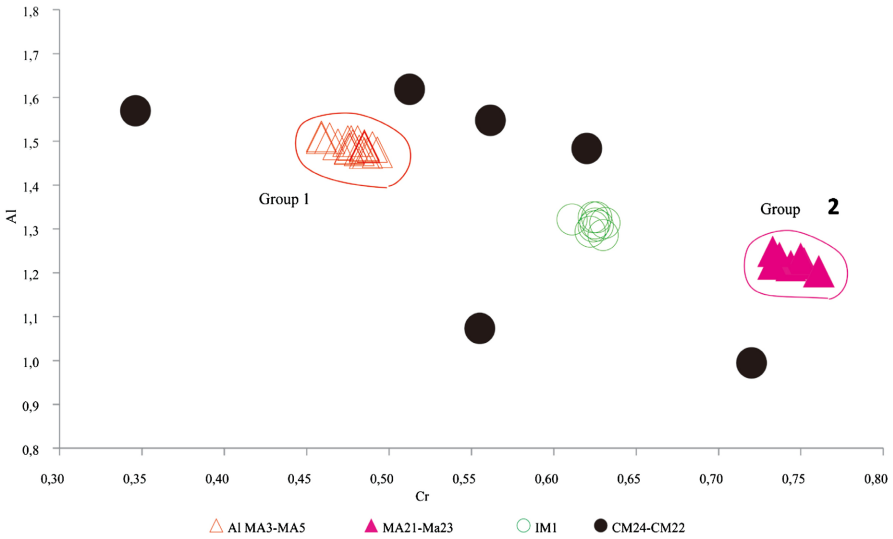

Figure 13. Al versus Cr diagram of spinels from spinel lherzolitic xenoliths in lava from Tertiary volcanism (IM1 and CM24 - CM22) and Quaternary volcanism Group 1 (MA3 - MA5) and Group 2 (MA21 - MA23).

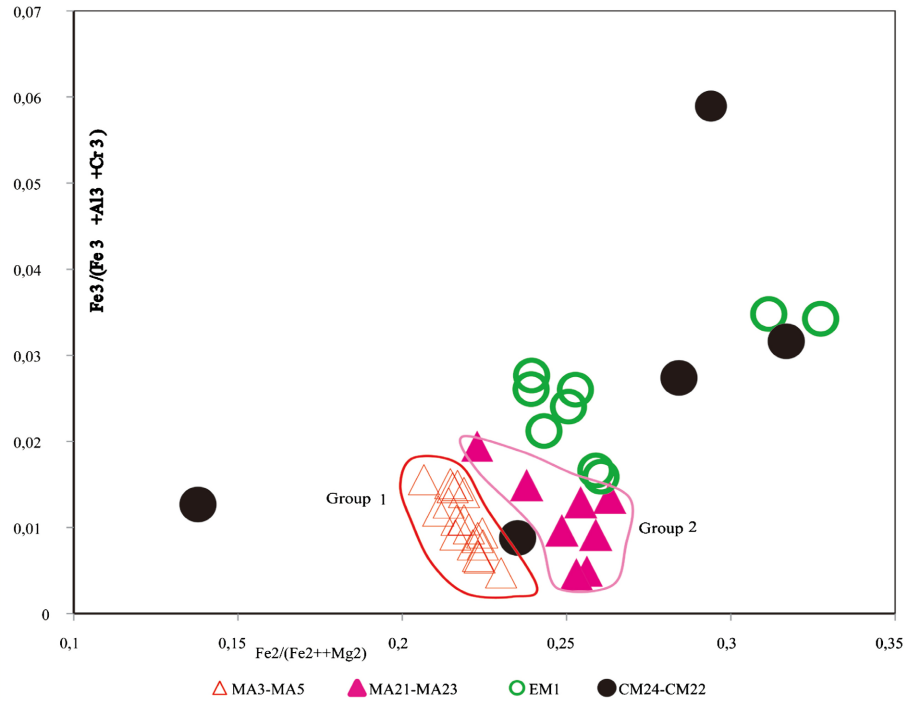

Figure 14. YFe ($Fe^{3+}/(Cr^{3+} + Al^{3+} + Fe^{3+})$ versus XFe ($Fe^{2+}/Fe^{2+} + Mg^{2+}$) diagram of spinels from spinel lherzolitic xenoliths in lavas from Tertiary volcanism (IM1) and (CM24 - CM22) and Quaternary volcanism Group 1 (MA3 - MA5 and Group 2 (MA21 - MA23).

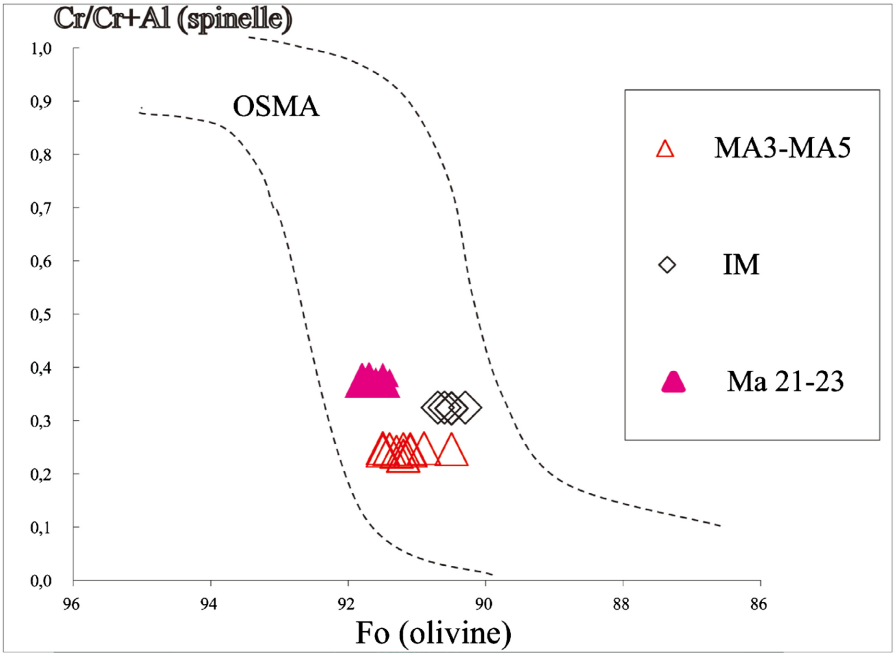

Figure 15. Cr/Cr + Al variations in spinel lherzolitic xenoliths as a function of Fo in spinel lherzolitic xenolith olivines in Tertiary and Quaternary lavas after Arai [29] OSMA: Olivine-Spinel Mantle Array: IM = Tertiary Xenoliths of the Magdalen Islands; MA, Ma 21, Ma23 = Quaternary spinel lherzolitic Xenoliths of the Mamelle.

The Cr/Cr + Al ratio (<0.5%) shows little variation in spinels. The low Ti (<0.063%) and Na (<0.158%) values in clinopyroxenes, and the low Ti (<0.003%) values in orthopyroxenes of spinel lherzolitic xenoliths, are compatible with a partial melting process of 10 to 15% [29], although the degree of partial melting may vary from one facies to another.

3.3. Geochemistry of Spinel Lherzolitic Xenoliths

3.3.1. Major Elements

Geochemical data obtained are shown in **Table 8**.

Quaternary xenoliths in (Mamelle) have MgO contents ranging from 43.13% to 46.486%, Al_2O_3 from 0.65% to 2.275%, Fe_2O_3 from 8.176% to 9.67%, CaO from 0.583% to 1.46%, TiO_2 from 0.007% to 0.09%, and Na_2O from 0.099% to 0.15%.

Compared to these Quaternary xenoliths, those found in Tertiary lavas have lower MgO (39.42% - 41.85%) and higher Fe_2O_3t (9.60% - 13.29%), CaO (1.75% - 2.63%), Na_2O (0.21% - 0.45%), K_2O (0.07% - 0.19%), and TiO_2 (0.12% - 0.31%).

The host lavas containing these tertiary and quaternary xenoliths are poorer in MgO (7.4% - 12.73%) and more enriched in Fe_2O_3t (9.81% - 13.41%), Al_2O_3 (11.51% - 15.04%), CaO (7.33% - 15.95%), TiO_2 (1.80% - 2.50%), and Na_2O (2.64% - 4.79%) [14].

Mg# differentiation index values (100*MgO/(MgO + Fe_2O_3t) are higher in xenoliths from Quaternary lavas (81.679% - 84.879%) than in those from Tertiary lavas (74.791% - 81.339%). These Mg# contents in xenoliths are higher than those in the host basalts (Mg# between 41.77% and 50.34%) [14].

Tertiary xenoliths are comparable to those described by McDonough [36], while quaternary xenoliths are similar to those described by several authors [26] [28] [37] [38] (**Figure 16**).

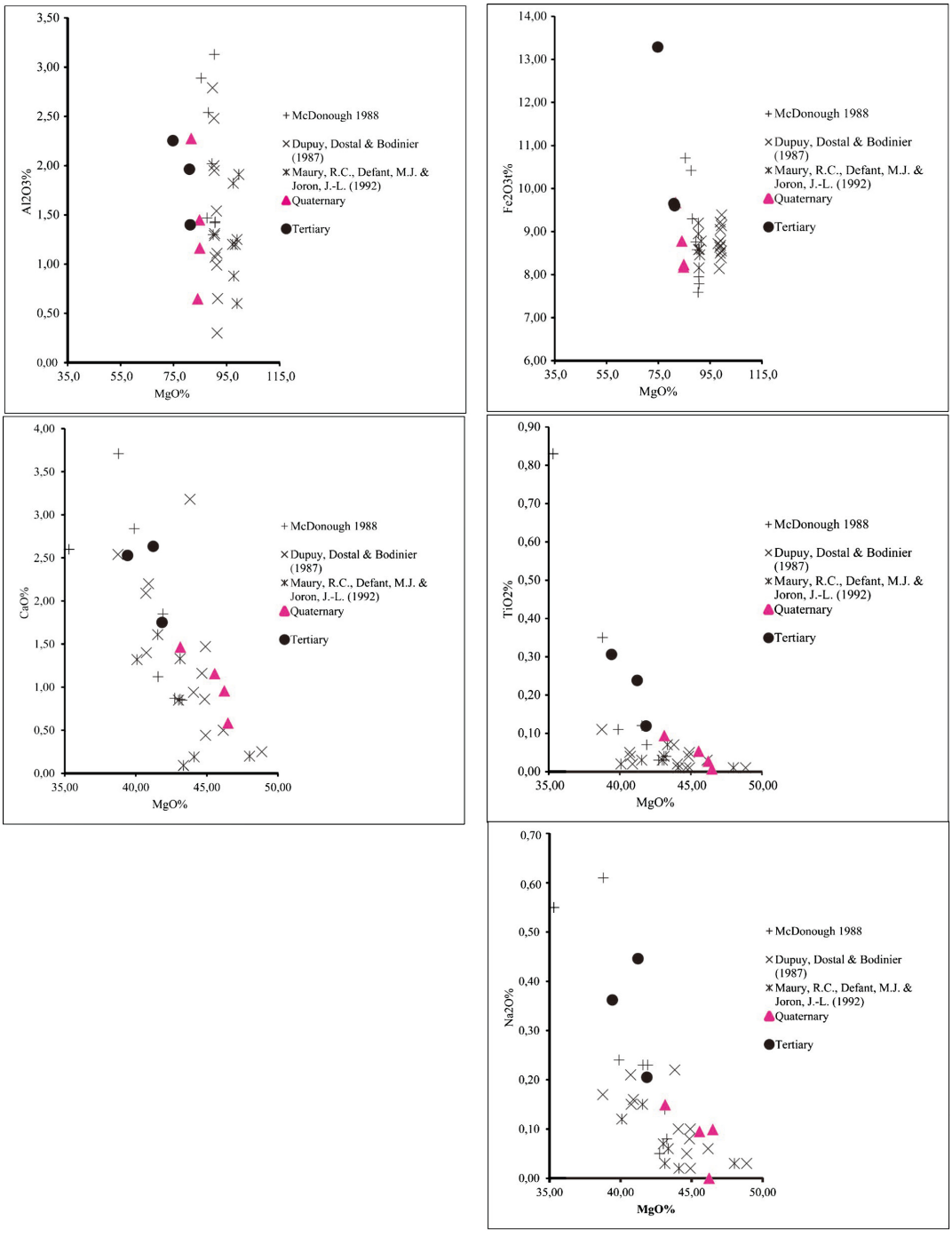

Figure 16. Al_2O_3, Fe_2O_3t CaO, TiO_2 and Na_2O versus MgO (wt%) diagrams of spinel lherzolitic xenoliths in Tertiary (Madelen Island and Cape Manuel) and Quaternary (Mamelle) lavas. Data are compared with GERM [26], McDonough [36], Downes and Dupuy [39], and Maury *et al.* [38].

Compared with the geotectonic sites defined by Bonati [25], the Quaternary

(Mamelle) and Tertiary (Manual Cape and Madeline Island) peridotite xenoliths are similar to the ocean basin xenoliths (Table 9) with a probable melting degree of 10% to 25% or passive margins with a probable melting degree of 10% to 15% [25].

Table 8. Major and trace elements in spinel lherzolitic xenoliths from Tertiary and Quaternary lavas.

	MA5	MA3	MA21	MA23	CM22	CM24	IM1
SiO_2	43.0	42.8	44.1	44.4	43.9	41.3	42.8
Al_2O_3	2.3	0.6	1.2	1.4	1.4	2.3	2.0
Fe_2O_3	9.7	8.8	8.2	8.2	9.6	13.3	9.7
MnO	0.1	0.1	0.1	0.1	0.1	0.2	0.1
MgO	43.1	46.5	46.2	45.6	41.9	39.4	41.2
CaO	1.5	0.6	1.0	1.2	1.8	2.5	2.6
Na_2O	0.1	0.1	<L.D.	0.1	0.2	0.4	0.4
K_2O	<L.D.	<L.D.	<L.D.	<L.D.	0.1	0.1	0.2
TiO_2	0.1	0.0	0.0	0.1	0.1	0.3	0.2
P_2O_5	0.1	0.1	0.1	0.0	0.1	0.2	0.1
PF	−0.3	−0.4	−0.5	−0.2	1.2	0.5	−0.1
Total	99.6	99.2	100.4	100.9	98.6	100.5	99.2
As	<L.D.	<L.D.	<L.D.	<L.D.	<L.D.	<L.D.	1.6
Ba	9.0	10.8	<L.D.	10.5	25.3	75.9	36.0
Be	<L.D.	<L.D.	<L.D.	<L.D.	<L.D.	<L.D.	<L.D.
Bi	<L.D.	<L.D.	<L.D.	<L.D.	<L.D.	<L.D.	<L.D.
Cd	<L.D.	0.4	<L.D.	<L.D.	<L.D.	0.2	<L.D.
Ce	1.1	1.2	0.5	2.2	5.9	16.0	7.0
Co	149.8	161.3	140.6	162.5	167.8	141.9	152.0
Cr	3184.0	3490.0	3457.0	4063.0	5500.0	3079.0	2947.0
Cs	<L.D.	<L.D.	<L.D.	<L.D.	<L.D.	<L.D.	<L.D.
Cu	6.3	4.7	6.2	64.4	13.2	32.7	31.9
Dy	0.2	0.0	0.1	0.1	0.3	0.8	0.6
Er	0.1	0.0	0.0	0.1	0.1	0.4	0.2
Eu	0.1	0.0	0.0	0.1	0.2	0.4	0.3
Ga	2.8	1.3	1.5	1.9	2.4	5.0	3.0
Gd	0.2	0.0	0.1	0.2	0.4	1.1	0.7
Ge	1.0	1.0	1.0	0.9	1.0	1.2	0.9
Hf	0.0	<L.D.	<L.D.	<L.D.	0.0	0.5	0.4
Ho	0.0	0.0	0.0	0.0	0.1	0.1	0.1
In	<L.D.	<L.D.	<L.D.	<L.D.	<L.D.	<L.D.	<L.D.
La	0.5	0.9	0.3	1.3	3.2	8.4	3.4
Lu	0.0	0.0	0.0	0.0	0.0	0.0	0.0

Continued

Mo	<L.D.	0.5	<L.D.	0.5	0.6	0.5	<L.D.
Nb	0.9	1.2	0.7	2.0	2.9	9.8	6.0
Nd	0.7	0.3	0.2	0.9	2.5	7.1	3.6
Ni	2178.0	2374.0	2190.0	2131.0	1984.0	1688.0	2100.0
Pb	<L.D.	<L.D.	<L.D.	<L.D.	<L.D.	4.9	<L.D.
Pr	0.1	0.1	0.1	0.3	0.7	1.8	0.9
Rb	0.7	0.8	0.7	1.4	3.1	5.2	5.9
Sb	<L.D.	<L.D.	<L.D.	<L.D.	<L.D.	<L.D.	<L.D.
Sm	0.2	0.1	0.1	0.2	0.5	1.4	0.8
Sn	<L.D.	0.9	<L.D.	0.2	0.3	0.4	0.3
Sr	13.6	25.9	4.0	17.3	74.3	127.3	67.8
Ta	0.3	0.4	0.2	0.6	0.7	0.9	0.9
Tb	0.0	<L.D.	0.0	0.0	0.1	0.2	0.1
Th	0.1	0.1	<L.D.	0.1	0.4	1.1	0.4
Tm	0.0	<L.D.	0.0	0.0	0.0	0.0	0.0
U	<L.D.	<L.D.	<L.D.	<L.D.	0.1	0.3	0.1
V	43.7	23.9	31.8	35.5	41.7	56.1	57.0
W	279.2	300.3	212.1	459.2	510.6	190.0	313.6
Y	1.2	<L.D.	0.2	0.6	1.2	3.6	2.6
Yb	0.1	0.0	0.0	0.1	0.1	0.3	0.2
Zn	59.5	54.7	48.1	54.3	73.1	118.8	66.7
Zr	4.3	3.6	1.7	4.0	7.7	23.1	19.4

Table 9. Variations in spinel lherzolitic xenoliths and oceanic peridotites from divergent to convergent zones after Bonatti [25].

Geotectonic settings	Total rock		Mineralogy			Melting ratio
	Al_2O_3 %	100 Mg/Mg + Fe	Olivine Fo	Orthopyroxene Al_2O_3 %	Spinel 100 Cr/Cr + Al	
Continental Rift	3.5 - 6	87 - 89	87 - 89.5	3.5 - 6	8 - 10	0%
Passive Margin	2.5	89.5	89 - 90	3.5 - 5	10 - 30	10% - 15%
Ocean basin	0.8 - 3	90 - 91.5	89 - 91,5	2.5 - 5	15 - 60	10% - 25%
active margin	0.5 - 0.8	92	91 - 92	0.5 - 2.5	50 - 80	50% - 80%
			this study			
Mamelle	0.6 - 2.3	81 - 85	89.1 - 91.8	3.58 - 3.78	23.3 - 38.7	
Madelen Island	1.96	81	90.3 - 91.8	3.52	31.6 - 32.9	
Manual Cape	1.3 - 2.3	74 - 82	75.9 - 92.4	-	18.1 - 44.3	

3.3.2. Trace Elements

Concentrations of compatible trace elements (Cr ranges from 2947 - 5500 ppm,

Ni from 1688 - 2374 ppm, Co from 140.6 - 167.8 ppm) are relatively high.

The Fe/Mn (64.5 to 72.55), Ni/Co (11.82 to 15.57), and Ni/Cr (0.36 to 0.71) ratios of the xenoliths studied are comparable to those of the primitive mantle (Fe/Mn = 54 to 68, Ni/Co = 16.7 to 19.3, and Ni/Cr = 0.72 to 1.07), the French Massif Central [39] (Fe/Mn = 55 to 69, Ni/Co = 17.7 to 20.3, and Ni/Cr = 0.82 to 1.17), but are also close to those of spinel peridotites [36] (Fe/Mn = 50 to 70, Ni/Co = 16 to 24, and Ni/Cr = 0.55 to 0.86) see [26].

The Rare Earth spectra of all the xenoliths studied show sub-parallel patterns with a progressive decrease from Light Rare Earth Elements (LREE) to Medium Rare Earth Elements (MREE) to Heavy Rare Earth Elements (HREE). Xenoliths in tertiary lavas show greater Rare Earth fractionation than those in quaternary lavas (**Figure 17**).

The ratios in quaternary xenoliths $[La/Sm]_N$ (1.8484 - 9.3225), [Sm/Yb]N (1.1315 - 2.4181), and $[La/Yb]_N$ (2.8171 - 20.2524) show wider variation than tertiary xenoliths, which have $[La/Sm]_N$ 2.8092 - 4.2411, $[Sm/Yb]_N$ 3.7943 - 5.0053, and $[La/Yb]_N$ 10.6589 - 20.7083, respectively. Such spectra show that these xenoliths come from a Rare Earth Depleted spinel lherzolite mantle source zone. Enrichment in Light Rare Earths relative to Heavy Rare Earths may result from contamination by the surrounding magma, which forms a glassy film along fractures and can contribute significantly to enrichment in these elements. This has been described in the case of peridotite xenoliths in alkaline basalts [40]. It may also be a characteristic feature of xenoliths if they represent cumulates derived from liquids enriched in Light Rare Earths [41], or if they result from cumulates formed from a liquid enriched and fractionated in Light Rare Earths for kimberlite nodules [41].

The low contents of incompatible elements (Ce, La), the high Ni and Cr contents, and the Mg/Mg + Fe ratio in both olivines and spinel lherzolitic xenoliths appear incompatible with the fractional crystallization process; they are more consistent with the partial melting process.

The low contents of Heavy Rare Earths may suggest that the source zone of these xenoliths is depleted in Heavy Rare Earths, such as spinel lherzolites.

The multi-element diagram (**Figure 18**), normalized to C1 chondrites [42], shows sub-parallel spectra reflecting enrichment in LILE (Rb, Sr, K) and HFSE (Zr, Ti, Y) with a positive Ta anomaly and a negative Hf anomaly. These variations, coupled with slight negative anomalies in Ba, Th, and Na, may indicate low partial melting of the source zone.

The distribution of normalized trace elements in early mantle xenoliths differs significantly from those in the host lavas (**Figure 19**), with the lavas being more enriched in rare earth elements than the xenoliths. The host lavas exhibit negative anomalies in K, Pb, P, and Zr, and positive ones in Sr and Nd, whereas the xenoliths have negative anomalies in K, Pb, U, and Y, and positive ones in Ta and P. These variations indicate that the trace element compositions of the xenoliths are not significantly affected by the host lavas. Variations in highly incompatible elements such as U and Rb, which are known to be mobile in subsurface environ-

ments, show that these elements are not significantly affected by post-magmatic or secondary alteration processes.

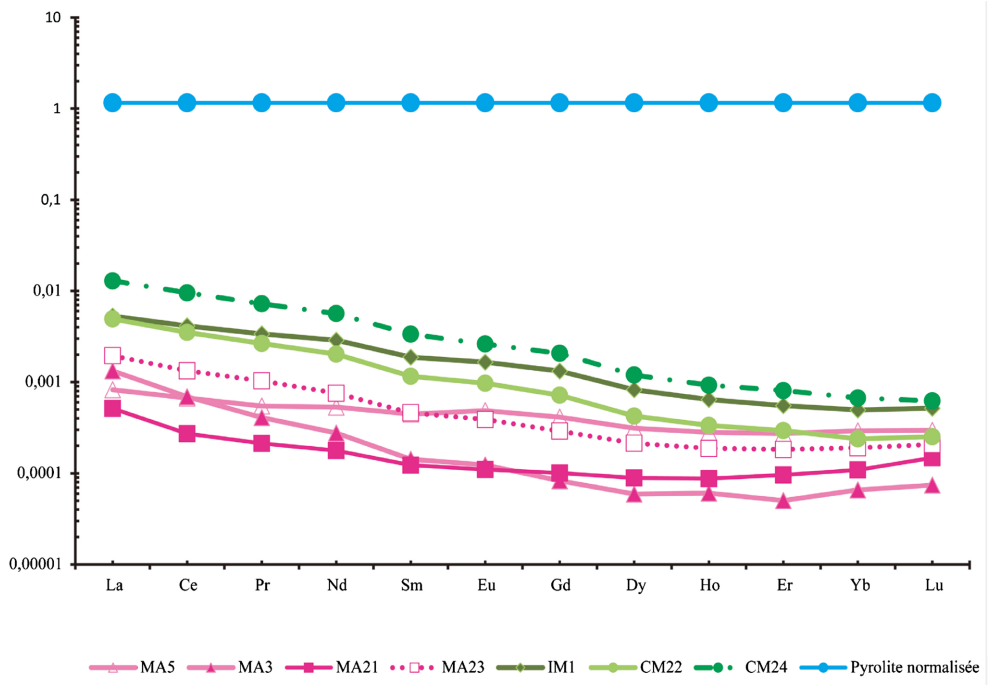

Figure 17. Rare Earth diagrams normalized to C1 chondrites [42] in the lherzolitic spinel xenoliths. Blue: Pyrolite Normalized. Green: Spinel lherzolitic xenoliths are present in the Tertiary lava of Madelen Island (IM1) and Manual Cape (CM22 and CM24). Pink: Spinel lherzolitic xenoliths in the Quaternary Mamelle lavas (MA3, MA5, MA21 and MA23).

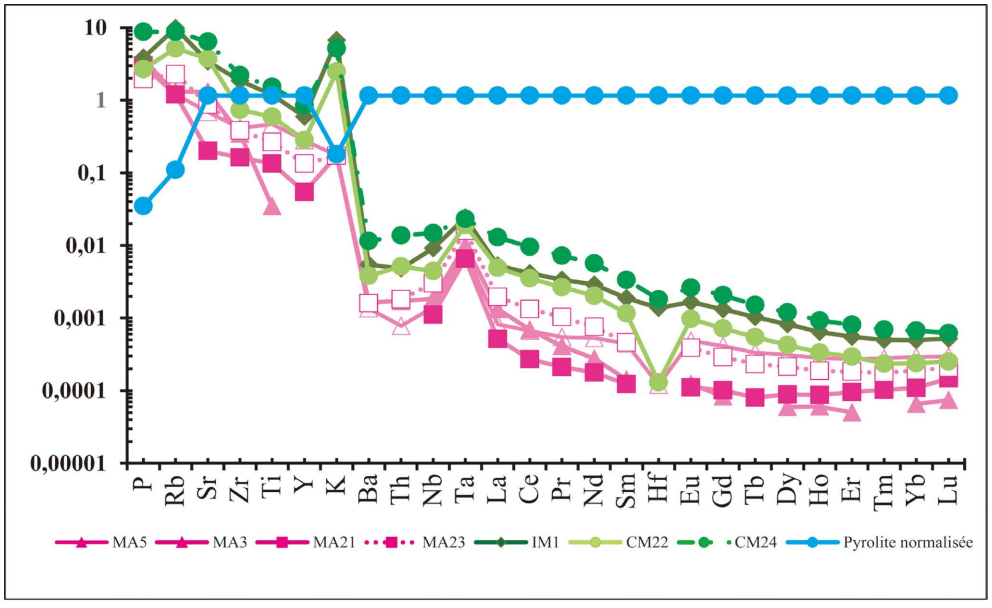

Figure 18. Multi-element diagrams normalized to C1 chondrites [42]. Blue: Pyrolite Normalized. Green: Spinel lherzolitic xenoliths in the Tertiary lava of Madelen Island (IM1) and Manual Cape (CM22 and CM24). Pink: Spinel lherzolitic xenoliths in the Quaternary Mamelle lavas (MA3, MA5, MA21 and MA23).

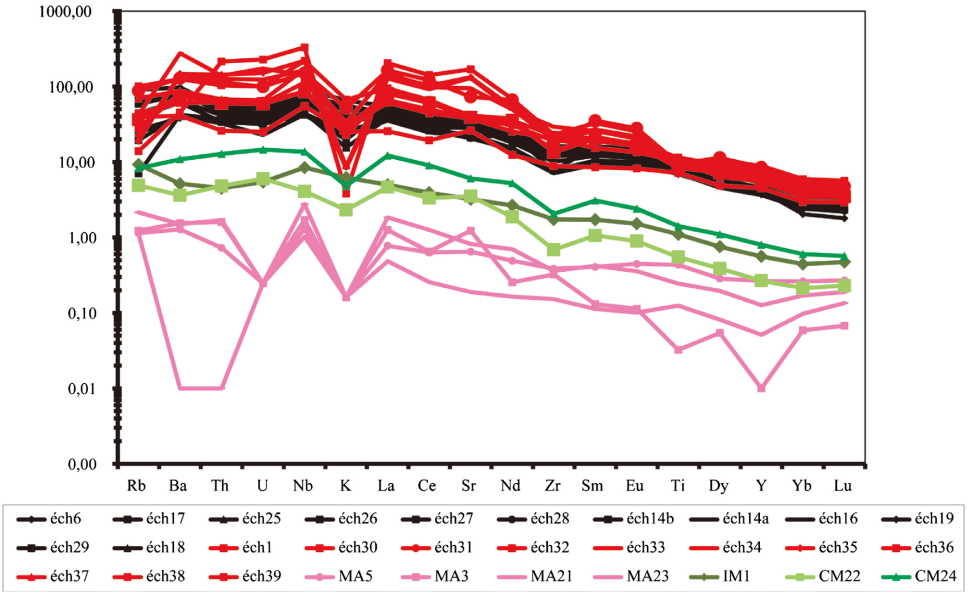

Figure 19. Multi-element diagrams of trace elements normalized to C1 chondrites [42] from spinel lherzolitic xenoliths compared with those from lavas. Red: Tertiary lavas: Ech 1 = Basanite of Madelen Island; ech30 = Nephelinites East Manual Cape; ech31 = Pegmatitoïde Manual Cape; ech32 = west Manual; ech33 = Basanite dyke Hinds Cape; ech34 = Nephelinites Hinds Cape; ech35 = Nephelinite microlitic Diokoul; ech36 = Pegmatitoïde Diokoul; ech37 = Basanite of Diack; ech38 = Dolérite of Diack; ech39 = Gabbros of Diack Black: Quaternary lavas: Ech 6 = Scoria; ech25 = First basanite flow; ech26 = Third basanite flow; ech27 = Fourth basanite flow; ech28 = Layens sanctuary basanite; ech17 = Glove finger basanite; ech18: Basanite from the Mermoz apparatus; ech19 = Dolerite thread; ech16 = Sheet cone dolerite; ech29 = Lower University dolerite; ech14a = Lower VDN dolerite; ech14b = Upper VDN dolerite; Green: Spinel lherzolitic xenoliths in Tertiary lavas: Madelen Island (IM1), Manual Cape (CM22 and CM24); Pink: Spinel lherzolitic xenoliths in Quaternary lavas: Mamelle (MA3, MA5, MA21 and MA23).

4. Conclusions and Perspectives

The spinel lherzolite xenoliths within the alkaline lavas from the Senegal Cape Verde Peninsula are characterized by irregular to sub-rounded shapes, fractured minerals, protogranular texture, inter-granular sliding, intense mineral cracking, basaltic infiltration, and a spinel structure. These observations suggest geochemical and thermodynamic disequilibrium of the spinel lherzolite xenoliths in contact with the host lavas and basaltic infiltrations contemporaneous with the eruption. This means that the spinel lherzolite xenoliths are mantle xenoliths transported by the ascending magma, and the temperature of the basaltic lavas was higher than that of the spinel lherzolite xenoliths when incorporated. The primary homogeneous assemblage (olivines, clinopyroxenes, orthopyroxenes, and spinels) is automorphic to subautomorphic, highly fractured, and develops triple junctions, reflecting the residual nature of xenoliths and their equilibrium in the host lavas. This is also confirmed by the precocious character of spinels.

The hypothesis of a mantle origin is supported by the high Fo (75.9 - 92.4) and NiO (0.039% - 0.442%) contents of the olivines, and the low contents of MnO (0.058% - 0.505%), CaO (0.0 - 1.352% wt.), and TiO_2 (0 - 0.108%). Spinels from

the Mamelle and Manual Cape xenoliths have low TiO_2 contents (0.08% - 0.27%), similar to typical mantle spinels (<0.2%). In contrast, the xenoliths from Madelen Island are richer in TiO_2 than those from the mantle (0.26% - 22.02%).

The mineralogical characteristics of the xenoliths studied are comparable to those of oceanic shelf basalt peridotites, oceanic hotspot peridotites, the sub-continental fertile peridotite group, and the island arc of Japan [29]. They fall within the domain of the olivine-spinel mantle (OSMA) and the domain of continental peridotites of the passive margin type, with a degree of melting between 10% and 15% [29].

The nature of OIB-type Cenozoic-hosted basalts suggests they may derive from the partial melting of a lherzolitic peridotite mantle source, comparable to those described in the Cameroon line [30] [43], Cape Verde Archipelago [44], and other mantle xenoliths [21] [31].

These xenoliths are characterized by a high degree of homogeneity in major and trace element compositions within the rocks. The Rare Earth spectra of the peridotites show little variability and are sometimes similar to early mantle estimates, which is also true for the magmatophilous major element compositions of the xenoliths analyzed. The Rare Earth spectra of xenoliths from the Senegal Cape Verde Peninsula are almost identical, with higher Rare Earth Element fractionation in xenoliths from Tertiary lavas than in Quaternary lavas. This indicates little or no contamination by the carrier basalts during the ascent of the xenoliths, and that the various mineral phases have remained largely undisturbed since their incorporation into the host basalt. The slight depletion of Light Rare Earth Elements relative to other Rare Earth Elements in xenoliths MA3 and MA21 suggests a partial melting episode, while the enrichment of Light Rare Earth Elements in other samples indicates metasomatism. The low fractionation of Heavy Rare Earth Elements indicates a partial melting episode in the spinel lherzolite facies, and the depletion suggests that the mantle beneath the Senegal Cape Verde Peninsula was originally strongly depleted. The spectra of Rare Earth Element peridotites and host lavas differ (**Figure 15**).

The spinel lherzolite xenoliths studied are comparable to those described in the alkaline volcanism of the Cameroon Volcanic Line and Cape Verde Archipelago. The xenoliths from the Cameroon Volcanic Line, characterized by the absence of garnet or primary plagioclase and metasomatic minerals, result from low partial melting of the Primitive Mantle at shallow depths within the lithosphere with mantle diapirism [43]. A low degree of partial melting in the Primitive Mantle is also determined in the Cape Verde Archipelago lithospheric mantle [44].

Consequently, the spinel lherzolite xenoliths in the Senegal Cape Verde Peninsula are slightly equilibrated with the host lava magma and are not purely crystallized from these magmas. However, they may still be enriched in light rare earth elements by magmatic infiltration. These characteristics suggest that the mantle beneath the Senegalese Cape Verde Peninsula is homogeneous in petrographic, mineralogical, and geochemical terms. This mantle can be considered locally

melted with a low degree of melt and was later affected by metasomatic processes through chemical enrichment. It was slightly enriched in rare earth elements, supporting the presence of homogeneous mantle diapirs along the Senegal-Cape Verde Peninsula.

The mantle diapirism model can be proposed to explain the origin of the Senegal Cape Verde Peninsula, similar to the Cameroon volcanic line [43] or Cape Verde Archipelago [44].

For future prospects, major and trace mineral elements, isotopic analysis, crystallization conditions, equilibrium temperatures, and fluid inclusions are required to better understand mantle evolution under the Senegal Cape Verde Peninsula.

Conflicts of Interest

The authors declare no conflicts of interest regarding the publication of this paper.

References

[1] Bellion, P. (1987) Histoire géodynamique post-paléozoïque de l'Afrique de l'Ouest d'après l'étude de quelques bassins sédimentaires (Sénégal, Taoudenni, Lullemmeden, Tchad). Thèse Doct. Es sciences, Univ. D'Avignon et des Pays du Vaucluse, 292 p.

[2] Bellion, Y. and Crevola, G. (1991) Cretaceous and Cainozoic Magmatism of the Senegal Basin (West Africa): A Review. In: Kampuzu, A.B. and Lubala, R.T., Eds., *Magmatism in Extensional Structural Settings*, Springer, 189-208. https://doi.org/10.1007/978-3-642-73966-8_8

[3] Crévola, G. (1975) Le volcanisme tertiaire et quaternaire de la presqu'île du Cap-Vert. IV: Quelques données sur les formations volcaniques de l'Ile aux Serpents. Bull. A.A.S.N.S., 33-42.

[4] Crévola, G., Cantagrel, J.M. and Moreau, C. (1994) Le volcanisme cénozoïque de la presqu'île du Cap-Vert (Sénégal): Cadre chronologique et géodynamique. Bull. Soc. Géol. France, 437-446.

[5] Gorodiski, A. (1952) Notice explicative de la carte géologique du Sénégal à 1/20000 (Feuille de Ouakam de Dakar). Bull. Dir. Mines, de l'A. O. F. (Dakar), 5-57.

[6] Crévola, G. (1980) Données nouvelles sur le volcanisme quaternaire de la tête de la presqu'île du Cap Vert (Sénégal). *Comptes Rendus de l'Académie des Sciences Paris*, *Série D*, **291**, 617-620.

[7] Debant, P. (1963) Les roches volcaniques récentes de la feuille au 1/20000 de Ouakam (République du Sénégal). *Annales de la Faculté des Sciences*, *Université de Dakar*, **10**, 79-154.

[8] Lo, P.G. (1988) Le volcanisme quaternaire du Sénégal occidental: Caractères pétrographiques, particularités géochimiques, implications pétrogénétiques.

[9] Bellion, Y. and Guiraud, R. (1984) Le bassin sédimentaire du Sénégal. Synthèse des con-naissances actuelles. In: BRGM et DMG Dakar, Eds., *Plan minéral de la république du Sénégal*, B.R.G.M. et D.M.G., Dakar, 4-63.

[10] Cantagrel, J.M., Crévola, G., Lapartient, J.R. and Tessier, F. (1980) Ages radiométriques K/Ar, pour le volcanisme de la presqu'île du Cap-Vert. *Comptes Rendus de l'Académie des Sciences*, 617-620.

[11] Cantagrel, J.M., Lapartient, J.R. and Tessier, F. (1978) Nouvelles données géochronologiques sur le volcanisme ouest africain. Bull. A.S.E.Q.U.A., 16-17.

[12] Dia, A. (1980) Contribution à l'étude Des Matériaux Volcaniques de La Presqu'île Du Cap Vert et Du Plateau de Thiès. Inventaire et Étude Préliminaire Des Sites. Mém. D. E. A. Fac. Sci. Dakar, Rap. 6 nvlle série.

[13] Fraudet, P. (1973) Contribution à l'étude des roches éruptives de la région de Thiès (Sénégal). Doc. Fac. Sci. Lyon, 15-86.

[14] Ndiaye, A. and Ngom, P.M. (2014) The Geodynamic Context of the Cenozoic Volcanism of the Cap-Vert Peninsula (Senegal). *International Journal of Geosciences*, **5**, 1521-1539. https://doi.org/10.4236/ijg.2014.512124

[15] Combier, M. (1952) Note sur les pegmatitoïdes de Gorée et de l'île des serpents. Bull. Dir. Mines. Afr. Occ. Fr. Dakar, 95-108, 5 pl.

[16] Tessier, F. (1950) Contribution à La Stratigraphie et à La Paléontologie de La Partie Ouest Du Sénégal. Thèse.

[17] Guieu, G. (1979) Comment se prolonge vers l'Ouest, le bassin Sénégalo-Mauritanien. *Comptes rendus de l'Académie des Sciences Paris*, **289**, 1117-1919.

[18] Liger, J.L. (1980) Structure Profonde Du Bassin Côtier Sénégalo-Mauritanien; Interprétation de Données Gravimétriques et Magnétiques. Thèse 3ème cycle.

[19] Lo, P.G., Dia, A. and Kampunzu, A.B. (1992) Cenozoic Volcanism in Western Senegal and Its Relationship to the Opening of the Central Atlantic Ocean. *Tectonophysics*, **209**, 281-291. https://doi.org/10.1016/0040-1951(92)90035-5

[20] Lompo, M. (1987) Méthodes et Étude de La Fracturation et Des Filons; Exemple de La Région Du Cap Vert (Sénégal). Mém. D. E. A.

[21] Mercier, J.C. and Nicolas, A. (1975) Textures and Fabrics of Upper-Mantle Peridotites as Illustrated by Xenoliths from Basalts. *Journal of Petrology*, **16**, 454-487. https://doi.org/10.1093/petrology/16.2.454

[22] Le Maitre, R.W., Streckeisen, A., Zanettin, B., Le Bas, M.J., Bonin, B., Bateman, P., Bellieni, G., Dudek, A., Efremova, S. and Keller Igneous Rocks: A Classification and Glossary of Terms (2002) Recommendations of the International Union of Geological Sciences Subcommission on the Systematics of Igneous Rocks. Cambridge University Press, 236 p.

[23] Le Maitre, R.W., Bateman, P., Dudek, A., Keller, J., Lameyre, J., Le Bas, M.J., Sabine, P.A., Schmid, R., Sorensen, H., Streckeisen, A., Woolley, A.R. and Zanettin, B. (1989) A Classification of Igneous Rock and Glossary of Terms. Recommendations of the International Union of Geological Sciences Subcommission on the Systematics of Igneous Rocks. Blackwell Sci. Publ., 193 p.

[24] Streckeisen, A. (1976) To Each Plutonic Rock Its Proper Name. *Earth-Science Reviews*, **12**, 1-33. https://doi.org/10.1016/0012-8252(76)90052-0

[25] Bonatti, E. and Michael, P.J. (1989) Mantle Peridotites from Continental Rifts to Ocean Basins to Subduction Zones. *Earth and Planetary Science Letters*, **91**, 297-311. https://doi.org/10.1016/0012-821x(89)90005-8

[26] GERM. http://www.earthref.org

[27] Morimoto, N. (1988) Nomenclature of Pyroxenes. *Canadian Mineralogist*, **27**, 143-156.

[28] McDonough, W.F. and Rudnick, R.L. (1998) Chapter 4. Mineralogy and Composition of the Upper Mantle. In: Hemley, R.J., Ed., *Ultrahigh-Pressure Mineralogy: Physics and Chemistry of the Earth's Deep Interior*, Mineralogical Society of America, Reviews in Mineralogy, 139-164.

[29] Arai, S. (1994) Compositional Variation of Olivine-Chromian Spinel in Mg-Rich Magmas as a Guide to Their Residual Spinel Peridotites. *Journal of Volcanology and Geothermal Research*, **59**, 279-293. https://doi.org/10.1016/0377-0273(94)90083-3

[30] Teitchou, M.I., Grégoire, M., Dantas, C. and Tchoua, F.M. (2007) Le manteau supérieur à l'aplomb de la plaine de Kumba (ligne du Cameroun), d'après les enclaves de péridotites à spinelles dans les laves basaltiques. *Comptes Rendus. Géoscience*, **339**, 101-109. https://doi.org/10.1016/j.crte.2006.12.006

[31] Cabanes, N. and Mercier, J. (1988) Chimie des phases minérales et conditions d'équilibre des enclaves de lherzolite à spinelle de Montferrier (Hérault, France). *Bulletin de Minéralogie*, **111**, 65-77. https://doi.org/10.3406/bulmi.1988.8071

[32] Carswell, D.A. (1980) Mantle Derived Lherzolite Nodules Associated with Kimberlite, Carbonatite and Basalt Magmatism: A Review. *Lithos*, **13**, 121-138. https://doi.org/10.1016/0024-4937(80)90013-4

[33] Dick, H.J.B. and Bullen, T. (1984) Chromian Spinel as a Petrogenetic Indicator in Abyssal and Alpine-Type Peridotites and Spatially Associated Lavas. *Contributions to Mineralogy and Petrology*, **86**, 54-76. https://doi.org/10.1007/bf00373711

[34] Zhou, M. and Robinson, P.T. (1994) High-CR and High-Al Podiform Chromitites, Western China: Relationship to Partial Melting and Melt/Rock Reaction in the Upper Mantle. *International Geology Review*, **36**, 678-686. https://doi.org/10.1080/00206819409465481

[35] Fisk, M.R., Bence, A.E. and Schilling, J. (1982) Major Element Chemistry of Galapagos Rift Zone Magmas and Their Phenocrysts. *Earth and Planetary Science Letters*, **61**, 171-189. https://doi.org/10.1016/0012-821x(82)90050-4

[36] McDonough, P. (1988) The Geology and Geophysics of the Murmungee Basin Ranodiorite and Surrounding Granites, Beechworth, NE Victoria. Unpublished BSc (Hons) Thesis, La Trobe University Bundoora Victoria.

[37] Dupuy, C., Dostal, J. and Bodinier, J.L. (1987) Geochemistry of Spinel Peridotite Inclusions in Basalts from Sardinia. *Mineralogical Magazine*, **51**, 561-568. https://doi.org/10.1180/minmag.1987.051.362.10

[38] Maury, R.C., Defant, M.J. and Joron, J. (1992) Metasomatism of the Sub-Arc Mantle Inferred from Trace Elements in Philippine Xenoliths. *Nature*, **360**, 661-663. https://doi.org/10.1038/360661a0

[39] Downes, H. and Dupuy, C. (1987) Textural, Isotopic and REE Variations in Spinel Peridotite Xenoliths, Massif Central, France. *Earth and Planetary Science Letters*, **82**, 121-135. https://doi.org/10.1016/0012-821x(87)90112-9

[40] Frey, F.A. and Green, D.H. (1974) The Mineralogy, Geochemistry and Origin of Iherzolite Inclusions in Victorian Basanites. *Geochimica et Cosmochimica Acta*, **38**, 1023-1059. https://doi.org/10.1016/0016-7037(74)90003-9

[41] Shimizu, N. (1974) An Experimental Study of the Partitioning of K, Rb, Cs, Sr and Ba between Clinopyroxene and Liquid at High Pressures. *Geochimica et Cosmochimica Acta*, **38**, 1789-1798. https://doi.org/10.1016/0016-7037(74)90162-8

[42] McDonough, W.F. and Sun, S. (1995) The Composition of the Earth. *Chemical Geology*, **120**, 223-253. https://doi.org/10.1016/0009-2541(94)00140-4

[43] Dagwai, N., Pierre, K., Bertrand, M.G.I., Gilles, C. and Ismaïla, N. (2024) Petrology of Spinel-Lherzolite Xenoliths from Mazélé and Others Northen Xenoliths Localities of Cameroon Volcanic Line: Exchange Reactions and Equilibrium State. *Open Journal of Geology*, **14**, 629-653. https://doi.org/10.4236/ojg.2024.145027

[44] Bonadiman, C., Beccaluva, L., Coltorti, M. and Siena, F. (2005) Kimberlite-Like Metasomatism and "Garnet Signature" in Spinel-Peridotite Xenoliths from Sal, Cape Verde Archipelago: Relics of a Subcontinental Mantle Domain within the Atlantic Oceanic Lithosphere? *Journal of Petrology*, **46**, 2465-2493. https://doi.org/10.1093/petrology/egi061